

See discussions, stats, and author profiles for this publication at: <https://www.researchgate.net/publication/272425000>

The Strengths and Weaknesses of NMR Spectroscopy and Mass Spectrometry with Particular Focus on...

Chapter *in* Methods in molecular biology (Clifton, N.J.) · April 2015

DOI: 10.1007/978-1-4939-2377-9_13

CITATIONS

21

READS

2,892

1 author:



Abdul-Hamid Emwas

King Abdullah University of Science and Technology

93 PUBLICATIONS 1,051 CITATIONS

SEE PROFILE

Some of the authors of this publication are also working on these related projects:



Development of a new biodegradable organosilica drug delivery systems (DDSs) [View project](#)



Ternary and quaternary chalcogenides [View project](#)

Metadata of the chapter that will be visualized online

Chapter Title	The Strengths and Weaknesses of NMR Spectroscopy and Mass Spectrometry with Particular Focus on Metabolomics Research	
Copyright Year	2015	
Copyright Holder	Springer Science+Business Media New York	
Corresponding Author	Family Name	Emwas
	Particle	
	Given Name	Abdul-Hamid M.
	Suffix	
	Division	Imaging and Characterization Core Lab
	Organization/University	King Abdullah University of Science and Technology
	City	Thuwal
	Country	Kingdom of Saudi Arabia
	Division	NMR Core Lab
	Organization/University	King Abdullah University of Science and Technology
	Street	Room 0149
	City	Thuwal
	Postcode	23955-6900
	Country	Kingdom of Saudi Arabia
	Email	abdelhamid.emwas@kaust.edu.sa

Abstract

Mass spectrometry (MS) and nuclear magnetic resonance (NMR) have evolved as the most common techniques in metabolomics studies, and each brings its own advantages and limitations. Unlike MS spectrometry, NMR spectroscopy is quantitative and does not require extra steps for sample preparation, such as separation or derivatization. Although the sensitivity of NMR spectroscopy has increased enormously and improvements continue to emerge steadily, this remains a weak point for NMR compared with MS. MS-based metabolomics provides an excellent approach that can offer a combined sensitivity and selectivity platform for metabolomics research. Moreover, different MS approaches such as different ionization techniques and mass analyzer technology can be used in order to increase the number of metabolites that can be detected. In this chapter, the advantages, limitations, strengths, and weaknesses of NMR and MS as tools applicable to metabolomics research are highlighted.

Keywords (separated by “ - ”)

NMR - MS - LC-MS - GC-MS - Metabolomics - Spectroscopy - Metabonomics

The Strengths and Weaknesses of NMR Spectroscopy and Mass Spectrometry with Particular Focus on Metabolomics Research 2 3 4

[AU1] Abdul-Hamid M. Emwas 5

Abstract 6

Mass spectrometry (MS) and nuclear magnetic resonance (NMR) have evolved as the most common techniques in metabolomics studies, and each brings its own advantages and limitations. Unlike MS spectrometry, NMR spectroscopy is quantitative and does not require extra steps for sample preparation, such as separation or derivatization. Although the sensitivity of NMR spectroscopy has increased enormously and improvements continue to emerge steadily, this remains a weak point for NMR compared with MS. MS-based metabolomics provides an excellent approach that can offer a combined sensitivity and selectivity platform for metabolomics research. Moreover, different MS approaches such as different ionization techniques and mass analyzer technology can be used in order to increase the number of metabolites that can be detected. In this chapter, the advantages, limitations, strengths, and weaknesses of NMR and MS as tools applicable to metabolomics research are highlighted. 7
8
9
10
11
12
13
14
15
16

Key words NMR, MS, LC-MS, GC-MS, Metabolomics, Spectroscopy, Metabonomics 17

1 Introduction 18

[AU2] Metabolomics is a technology-driven approach whereby recent developments in analytical tools, software, and statistical data analysis push the field forwards. Various analytical techniques have been used, but nuclear magnetic resonance (NMR) and mass spectrometry (MS) are the most common analytical tools in metabolomics research [1–14]. The high reproducibility of NMR-based techniques and the high sensitivity and selectivity of MS-based techniques mean that these tools are superior over other analytical techniques. Figure 1 shows the increase in the number of both NMR-based and MS-based metabolomics publications during the past 12 years. 19
20
21
22
23
24
25
26
27
28

Metabolomics analyses can be separated into the categories of targeted or untargeted analysis. Untargeted analysis focuses on the metabolic profiling of the total complement of metabolites 29
30
31

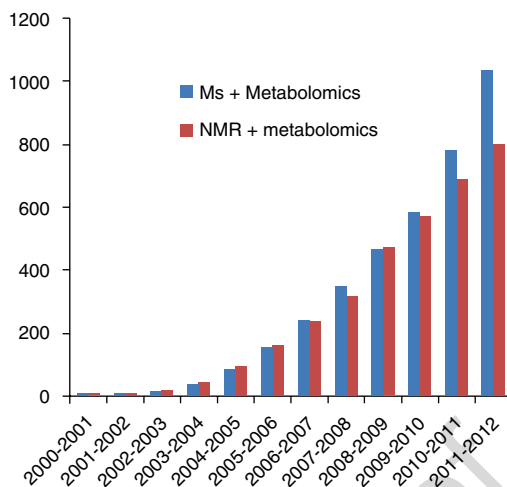


Fig. 1 Number of NMR metabolomics and MS metabolomics publications; literature review was conducted using Web of Knowledge (<http://apps.webofknowledge.com>) with the keywords (a) (metabolomics and NMR) and (b) (metabolomics and MS)

32 (“fingerprint”) in a sample. NMR is commonly used in metabolomics
 33 fingerprinting studies. The targeted metabolomics approach
 34 focuses on the quantification and identification of selected meta-
 35 bolites, such as those involved in a particular metabolic pathway
 36 or others as the direct product of drug administering or of food
 37 intake. In targeted analysis, the metabolites under investigation
 38 are usually known, and the preparation of samples can be adjusted
 39 to reduce the effects of interference from associated metabolites.
 40 An MS-based metabolomics approach is usually the optimum
 41 method for targeted analysis.

42 Continuous development of MS methodology and machinery
 43 presents a highly specific analytical tool that can provide chemical
 44 information such as accurate mass, isotope distribution patterns for
 45 the determination of elemental formulae, structural elucidation
 46 though the characteristics of parent and fragment ions, identifica-
 47 tion of chemicals using spectral matching to authentic compound
 48 data, and comparative concentration levels of different chemicals
 49 in mixed samples. In fact, MS-based metabolomics techniques pro-
 50 vide an exceptional combination of sensitivity and selectivity offer-
 51 ing a powerful platform for a wide range of metabolomics research.
 52 Compared with NMR spectroscopy, MS is superior in allowing
 53 analysis of secondary metabolites where the detection level is of
 54 picomole to femtomole [15, 16]. Moreover, the different MS
 55 technologies provide an array of operational principles that can be
 56 applied, such as different ionization techniques, so increasing the
 57 number of metabolites that can potentially be detected.

58 The high reproducibility along with the nondestructive and non-
 59 invasive characteristics of NMR spectroscopy represents significant

advantages for employing NMR in metabolomics research. Further, NMR can be employed for *in vivo* studies, referred to as magnetic resonance spectroscopy (MRS); any *in vitro* metabolite pathway investigated by NMR spectroscopy can be pursued by *in vivo* studies using MRS. An NMR-based metabolomics approach involving isotopically labeled nuclei such as ^{13}C and ^{15}N can be used to obtain useful information about the balance of metabolites in a biological system and to monitor the flow of compounds through metabolic pathways. The high number of metabolites that can be detected simultaneously in a short time period of only a few minutes represents further advantage of using NMR spectroscopy in metabolomics research. For example, a single proton NMR spectrum can quantify around 100 metabolites in a sample of human urine, this providing a comprehensive picture of human metabolic status at a given point in time [17]. Moreover, high-resolution magic-angle spinning (HRMAS) NMR spectroscopy can be used in the study of intact tissue samples whereby metabolites present in a tissue can be detected without the need for pre-preparation steps such as extraction [18–24].

Finally, it is crucial to remember that there is no single analytical platform that can perform a complete quantification and identification of all molecules within a sample. Table 1 demonstrates the advantages and the limitations of NMR spectroscopy compared to MS spectrometry. Thus, employing different techniques such as different ionization methods coupled with liquid chromatography–mass spectrometry (LC-MS) and gas chromatography–mass spectrometry (GC-MS) in addition to one- and two-dimensional NMR experiments is necessary to maximize the identification of different metabolites within a complex sample. For example, Wishart et al. employed different analytical platforms such as NMR, GC-MS, direct flow injection mass spectrometry (DFI/LC-MS/MS), inductively coupled plasma mass spectrometry (ICP-MS), and high-performance liquid chromatography (HPLC) to identify the human urine metabolome. The results show that a total of 209 different metabolites can be identified by NMR, in addition to 179 by GC-MS, 127 by DFI/LC-MS/MS, 40 by ICP-MS, and 10 by HPLC [25].

In this chapter, the advantages, limitations, strengths, and weaknesses of NMR and MS as tools applicable to metabolomics research are highlighted.

2 Materials

Compared with MS, NMR spectroscopy requires highly skilled and trained manpower operators, and it is more expensive to purchase and maintain; it also demands a large space for the instrumentation (Fig. 2). Consequently, MS instruments are much more commonly found in clinical centers and hospitals compared with NMR spectrometers.

t1.1 **Table 1**
 t1.2 **The advantages and limitations of NMR spectroscopy and MS spectrometry as an analytical tool for**
 t1.3 **metabolomics research adapted from ref. [14]**

[AU3]

t1.4		NMR	Mass spectrometry
t1.5	Sensitivity	Low but can be improved with higher field strength, cryo- and microprobes, and dynamic nuclear polarization	High and detection limit reach nanomolar
t1.6			
t1.7			
t1.8	Selectivity	Even though few selective experiments are available such as selective TOCSY, it is in general used for nonselective analysis	Can be used for both selective and nonselective (targeted and nontargeted) analyses
t1.9			
t1.10			
t1.11			
t1.12	Sample measurement	All metabolites that have NMR concentration level can be detected in one measurement	Usually need different chromatography techniques for different classes of metabolites
t1.13			
t1.14			
t1.15	Sample recovery	Nondestructive; sample can be recovered and stored for a long time; several analyses can be carried out on the same sample	Destructive technique but need a small amount of sample
t1.16			
t1.17			
t1.18			
t1.19	Reproducibility	Very high	Moderate
t1.20	Sample preparation	Need minimal sample preparation	More demanding; needs different columns and optimization of ionization conditions
t1.21			
t1.22			
t1.23	Tissue samples	Yes, using HRMAS NMR tissue samples analyzed directly	No, requires tissue extraction
t1.24			
t1.25	Number of detectable metabolites in urine sample	40–200 depending on spectral resolution	Could be more than 500 using different MS techniques
t1.26			
t1.27			
t1.28	Target analysis	Not relevant for targeted analysis	Superior for targeted analysis
t1.29	In vivo studies	Yes—widely used for ^1H magnetic resonance spectroscopy (and to a lesser degree ^{31}P and ^{13}C)	No—although suggestion that desorption electrospray ionization (DESI) may be a useful way to sample tissues minimally invasively during surgery
t1.30			
t1.31			
t1.32			
t1.33			

106 **2.1 Samples** Different biological samples are commonly used in metabolomics
 107 analysis including:
 108 – Bio-fluids.
 109 – Cell extracts.
 110 – Bacterial extracts.
 111 – Animal/human intact tissues.
 112 – Plant extracts.



this figure will be printed in b/w

Fig. 2 Typical NMR laboratory (KAUST NMR laboratory) where sufficient, separated space is required for location of NMR spectrometer (*top*); GC-MS where the GC-MS is usually small enough to be allocated on lab bench top (*bottom*)

[AU4]

2.2 Chemicals

1. The chemicals most commonly used in metabolomics analyses include HPLC grade solvents such as methanol, ethanol, chloroform, acetonitrile, and isopropanol. 113
114
115
2. Phosphate buffer is usually required for NMR analysis. 116
3. Solvents usually contain hydrogen atoms and the solvent ¹H NMR peak would overwhelm the solute ¹H peaks. 117
118
Consequently, deuterated solvents should be used for NMR 119

120 measurements; those most frequently used in metabolomics
121 studies are D₂O or (90:10 H₂O: D₂O) for polar metabolites
122 and CDCl₃ for lipid samples. In the case of strong solvent
123 residual peaks such as (90:10 H₂O: D₂O), the “solvent sup-
124 pression” experimental technique would be necessary to sup-
125 press the residual solvent peak.

126 4. References for NMR spectra: 4,4-dimethyl-4-silapentane-1-
127 sulfonic acid (DSS) or its sodium salt and 3-trimethylsilylpro-
128 pionic acid (TSP) are normally used for samples dissolve in
129 D₂O or 90:10 H₂O: D₂O, and tetramethylsilane (TMS) is the
130 most commonly used in organic solvents such as chloroform.

131 2.3 NMR Equipment

132 1. NMR magnets: Even though an ultrahigh magnetic field NMR
133 spectrometer, such as one set at 950 MHz, will offer better
134 resolution and higher sensitivity, such equipment is prohibi-
135 tively expensive and the maintenance is similarly costly.
136 Consequently, most NMR-based metabolomics studies have
137 been conducted using 600 and 500 MHz NMR spectrometers
138 that are commonly available in research institutes and offer a
139 good compromise between resolution, sensitivity, and cost.

140 2. NMR probes: Different NMR probes can be used for particu-
141 lar applications and for the detection of different nuclei.
142 Examples of commercial NMR probes that have commonly
143 been used in metabolomics research include:

144 (a) Double Resonance Broad Band Probes (BBO and BBOF)
145 often called Broad Band Inverse Probes. These are widely
146 used in experiments such as heteronuclear 2D experiments
147 involving single-quantum coherence (HSQC), heteronu-
148 clear multiple-quantum correlation (HMQC), and hetero-
149 nuclear multiple bond correlation (HMBC).

150 (b) Triple Resonance Broad Band Probe (TBI).
151 TBI can be used for all BBO applications, the extra chan-
152 nel bringing the advantage of being able to study another
153 X-nucleus, so providing the capability for study of organo-
154 metallic compounds and metalloproteins using ¹H, ¹³C,
155 and another metal-nucleus.

156 (c) Double Resonance Broadband Probe (BBI). Tunable to a
157 wide range of frequencies; used for detection of multinu-
158 clear experiments optimized for ¹H applications.

159 (d) Triple Resonance Broad Band Probe (TBO). TBO probe
160 has features similar to those of BBI probe but with one
161 extra channel.

162 (e) Triple Resonance Probe (TXI). Provides the opportunity
163 to pulse for up to three or four nuclei in one experiment;
164 used extensively for NMR structural determination of bio-
165 logical macromolecules.

- (f) Triple Resonance CryoProbe (TCI) (used mainly for protein applications but can also be used for metabolomics). The Probe is composed of three completely independent channels (in addition to a lock channel) that can be used for simultaneous decoupling on multiple nuclei, such as ^{15}N and ^{13}C . It is a powerful probe for multidimensional experiments, whereby pulsing up to four nuclei in one experiment is possible. Consequently, it is used mainly for NMR structural determination of biological macromolecules such as proteins.
- (g) MicroProbes (1 mm TXI, 1.7 mm TXI)—small volume probes (useful for samples of a small size).

2.4 MS Equipment

1. MS components: the MS instrument consists of three major components.
 - (a) *Ion source*: ionization part (produces gaseous ions).
 - (b) *Analyzer*: main function is to separate ions into distinctive mass components on the basis of mass-to-charge ratio (m/z).
 - (c) *Detector system*: detects ions based on their m/z and records relative abundance of each resolved ion.

The MS instrument also has other important components including a system to insert samples into the ion source and a computer to capture and analyze the data, as well as compare the spectra to reference MS database libraries. There are several ionization methods including EI (electron impact), CI (chemical ionization), MALDI (matrix-assisted laser desorption ionization), ESI (electrospray ionization), FAB (fast-atom bombardment), SIMS (resonance ionization), PD (plasma-desorption ionization), LIMS (laser ionization), and RIMS (resonance ionization). Application of each of these methods brings its own advantages and limitations. Sample analysis could be carried out using different types of analyzer such as time of flight (TOF), quadrupole, ion trap, magnetic sector, and Fourier transform mass spectrometry. It is beyond the scope of this chapter to give a detailed description of the application, advantages, and disadvantages of each method of ionization or mass analysis. Examples of LC-MS and GC-MS equipments that are available in our analytical core lab are presented in the following sections.
2. LC-MS equipment.
 - (a) TSQ Vantage, triple quadrupole MS.
 - (b) Loading pump, transcend system.
 - (c) Valve interface model.
 - (d) Accela PDA detector.
 - (e) CTC autosampler equipped with injector valve.

- 210 3. GC-MS equipment.
211 (a) 7890 GC.
212 (b) 7683 Autosampler.
213 (c) 5975 C quadrupole MSD.
214 (d) Trace GC ultra.
215 (e) Triplus autosampler.
216 (f) TSQ Quantum, triple quadrupole MS.
217 (g) Microtof II MS.
218 (h) GC Capillary Column: DB-5MS.

219 3 Methods

220 3.1 NMR 221 Spectroscopy

222 NMR spectroscopy is a powerful analytical tool that has been used
223 mainly in chemistry for the identification and quantification of the
224 chemical composition of a given sample. The applications of NMR
225 spectroscopy are not limited to liquid samples but can also be used
226 on solid [26–31], gas phase [32–36], and tissue samples [28, 29,
227 37–49]. Moreover, as well as its main applications in molecular
228 identification and structural elucidation, NMR can also be used to
229 study the physical and chemical properties of molecules, such as
230 electron density and molecular dynamics [50–57]. Consequently,
231 NMR has become the main tool for structural biology studies as it
232 enables researchers to study molecular structures as well as molecu-
233 lar dynamics under biological conditions. Moreover, NMR spec-
234 troscopy has been employed in a wide range of research areas
235 including structural biology, organic chemistry, inorganic chemis-
236 try, biochemistry, physics, biology, polymers, and drug discovery
237 [9, 41, 58–75]. NMR spectroscopy has been proposed as one of
238 the most relevant methods in metabolomics applications, for
239 example, as powerful diagnostic method for a wide range of human
240 diseases [11, 14, 76–87]. Low sensitivity is the inherent disadvan-
241 tage and the foremost challenge for the application of NMR in
242 biomedical research. Continuous developments in the relevant
243 machinery such as a higher magnetic field strength [88], cryogeni-
244 cally cooled probes [89], and microprobes [90] have significantly
245 enhanced the sensitivity of NMR. The dynamic nuclear polariza-
246 tion (DNP) approach is one of the most efficient developments
[91] that has been used successfully to enhance NMR sensitivity in
imaging and spectroscopy [92–95].

247 3.1.1 High-Resolution 248 Magic-Angle Spinning 249 (HRMAS) NMR 250 Spectroscopy

The applications of NMR spectroscopy are not limited to liquid
and solid samples, but extend to intact tissue samples with use of
high-resolution magic-angle spinning (HRMAS) NMR spectros-
copy. By spinning samples at an angle of 54.74° —the “magic

angle”—to the magnetic field and at high speed, spectra can be obtained with a resolution comparable to that of solution-state NMR spectra. Using this method, the chemical composition of tissue samples can be detected spontaneously without the need for pre-preparation steps such as extraction [18, 96]. In an NMR-based metabolomics approach, this technique is helpful in offering a correlation between the metabolic profiling of bio-fluids and the histology of specific tissues. Consequently, HRMAS NMR spectroscopy has been used to study the metabolomic balance of small intact tissue samples [97] including brain [98], kidney [99], liver [100], and testicular tissues [101]. HRMAS has recently been used in meningioma biopsies as a potential diagnostic tool for the differentiation of typical meningiomas and benign tissues [102]. Recently, Ying-Lan Zhao and coworkers have employed HRMAS spectroscopy in conjunction with principal component analysis (PCA), partial least squares discriminant analysis (PLS-DA), and orthogonal projection to latent structure with discriminant analysis (OPLS-DA) to investigate the metabolic profile of human rectal cancer tissue collected from 127 patients and compare these with 47 samples collected from healthy control subjects [103]. The results revealed a clear separation between the samples from patients and those from the healthy control subjects. Several distinguishing metabolites were identified and correlated to different stages of rectal cancer tissues, so demonstrating the possibility of using metabolite biomarkers to follow the progression of rectal cancer. Moreover, a total of 38 differential metabolites were successfully identified, and 16 of them were found to be closely correlated with a particular stage of rectal cancer. The results demonstrate that, compared with healthy control samples, the concentration levels of several metabolites including lactate, threonine, acetate, glutathione, uracil, succinate, serine, formate, lysine, and tyrosine are found to be elevated in cancer tissue samples from patients, whereas the levels of other metabolites such as taurine, creatine, betaine, myo-inositol, phosphocreatine, and dimethylglycine are found to decrease [103].

[AU5]

3.1.2 One-Dimensional (1D) NMR Spectroscopy

Although NMR spectroscopy has been used in numerous multidimensional experiments with different detectable nuclei, one-dimensional (1D) proton (^1H) NMR remains the most usable and useful technique, especially for metabolomics studies. However, due to the narrow range of chemical shift (10 ppm), ^1H NMR spectra from overlapped signals usually persist, and this leads to uncertainty in the spectral assignments. Figure 3 shows the proton NMR spectrum of a sample composed of two simple molecules, *n*-propanol and *n*-butanol. As can be seen from the figure, the signals for the methyl groups for both *n*-propanol and *n*-butanol are observed at 0.92 ppm as an overlapped signal and cannot be

this figure will be printed in b/w

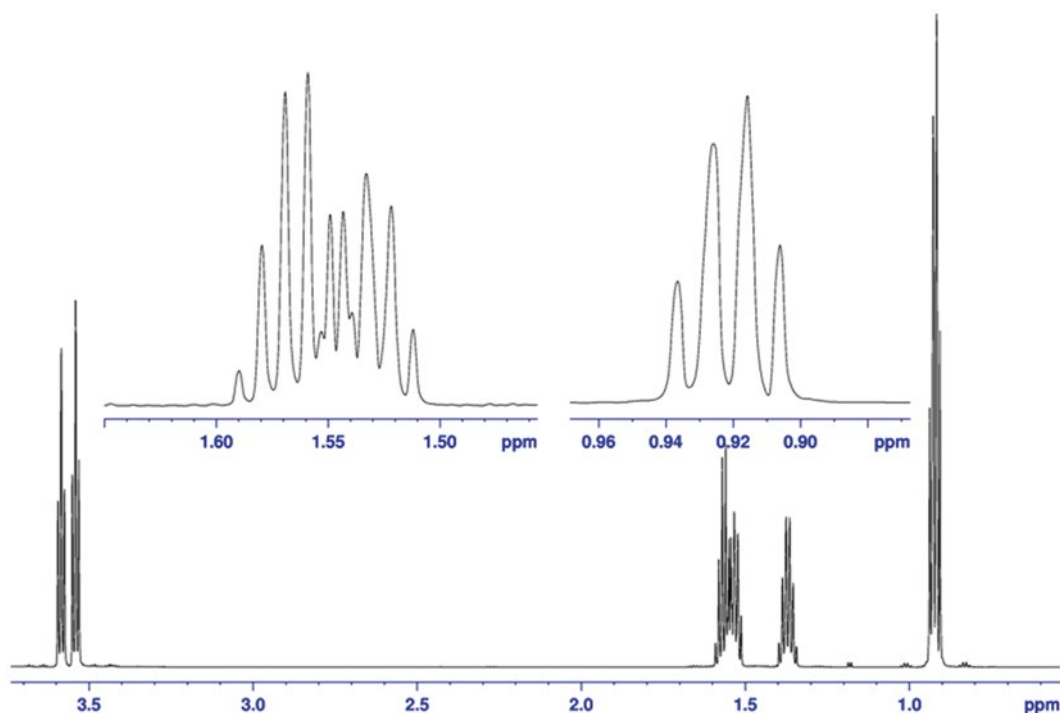
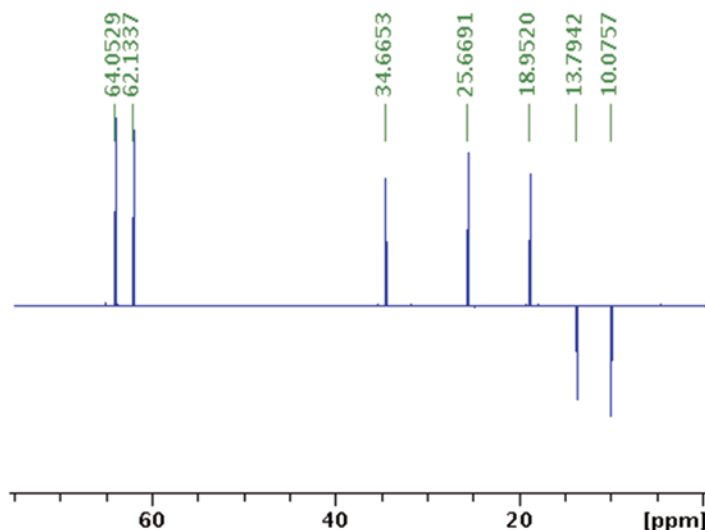


Fig. 3 700 MHz proton NMR spectrum of a sample composed of two simple molecules, *n*-propanol and *n*-butanol, dissolved in CDCl₃ recorded at 298 K

297
298
299
300
301
302
303
304
305
306
307
308
309
310
311
312
313
314
315
316
317
318

resolved by simple 1D NMR spectroscopy. Moreover, overlapping signals were also obtained at 1.55 ppm. These overlapping signals are related to the -CH₂-groups from the two molecules, but it is not possible to ascribe a particular signal to a particular molecule based on the simple 1D proton NMR spectrum. Other nuclei such as carbon and nitrogen have a wider range of NMR chemical shift but bring other limitations. For example, one-dimensional phosphorous (³¹P) NMR spectroscopy has a few advantages such as the 100 % natural abundance of the ³¹P nuclei, a wide chemical shift range, and high sensitivity. Thus, ³¹P NMR spectroscopy is commonly used to study phospholipids and metabolites involved in energy metabolism [104, 105]. However, the fact that most metabolites do not contain phosphorus represents the main limitation of ³¹P NMR spectroscopy. Generally, the spectral width of one-dimensional carbon (¹³C) NMR spectra is more than 200 ppm leading to wider spectral dispersion. ¹³C NMR spectroscopy is particularly informative in molecular identification and for structural elucidation. However, the low natural abundance of the ¹³C nuclei (1.1 %) as well as a low sensitivity has hindered the use of this isotope in NMR-based metabolomics applications. Different NMR approaches have been developed to enhance the ¹³C NMR signals. For example, Distortionless Enhancement by Polarization Transfer



this figure will be printed in b/w

Fig. 4 DEPT-135 ^{13}C NMR spectrum of a mixed sample composed of *n*-propanol and *n*-butanol in CDCl_3 at 298 K. The CH_3 signals in the opposite direction of the CH_2 signals providing a powerful approach to resolve the CH_3 signals from CH_2 ones are illustrated

(DEPT) is a powerful means of increasing the sensitivity of NMR spectra whereby the ^{13}C signal intensity can be enhanced by a factor of four. DEPT NMR experiments are also useful for distinguishing between CH_2 and (CH , CH_3), as the ^{13}C NMR spectrum of DEPT-135, for instance, yields CH_2 peaks with a negative intensity and CH and CH_3 peaks with a positive intensity (Fig. 4).

^{15}N NMR spectroscopy is very useful in structural biology including the study of proteins, RNA, and DNA structure and dynamics and also investigation of protein–metal coordination, protein–protein, and protein–ligand interaction [106–112]. However, due mainly to the low natural abundance of ^{15}N at only 0.37 % and a low sensitivity, this approach is expected to be less useful in metabolomics studies.

3.1.3 Two-Dimensional (2D) NMR Spectroscopy

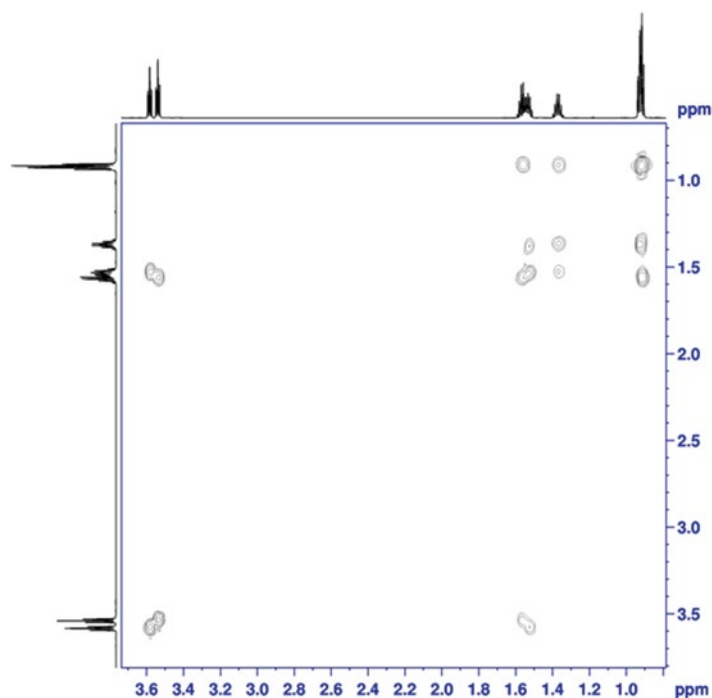
Two-dimensional (2D) NMR spectroscopy can be used to overcome the problem of overlapping resonances in proton 1D NMR spectra, leading to the detection and assignment of a greater number of metabolites than is possible with the 1D method. 2D NMR spectroscopy is based on through space spin coupling or through bond coupling, the former being used mainly for structural elucidation and the latter for molecular identification. Through bond correlation, NMR spectroscopy divides into two main categories: homonuclear, being mostly (^1H – ^1H) such as correlation spectroscopy (COSY) [113] and total correlation spectroscopy (TOCSY) [114], and heteronuclear, such as (^1H – ^{13}C). Both the homonuclear

343 and heteronuclear categories have been used in NMR-based
344 metabolomics studies for signal isolation and to support the assign-
345 ment of metabolites [115–119]. Other 2D methods, such as two-
346 dimensional J-resolved NMR spectroscopy (J-Res) [120], and
347 diffusion-ordered spectroscopy (DOSY) [121] have been used in
348 NMR-based metabolomics studies. A combination of COSY and
349 DOSY was employed to study metabolic changes in dystrophic
350 heart tissue for samples collected from a mouse model of muscular
351 dystrophy [122]. Heteronuclear 2D experiments involving single-
352 quantum coherence (HSQC), heteronuclear multiple-quantum
353 correlation (HMQC), and heteronuclear multiple bond correla-
354 tion (HMBC) have a high degree of resolution in the second
355 dimension mostly using (^{13}C) and have been employed for metab-
356 olite discrimination and identification [123].

357 Although 2D NMR experiments improve the dispersing of
358 the NMR signals, increased acquisition time, data size, and com-
359 plexity in data analysis limit frequent use of this approach. However,
360 the continuous development of NMR machinery and new faster
361 NMR method of signal acquisition and data processing are lead-
362 ing to the increased use of 2D techniques in metabolomics studies
363 [113, 124–126].

364 3.1.4 Correlation 365 Spectroscopy (COSY)

366 COSY was the first technique of 2D homonuclear correlation spec-
367 troscopy and has been used over many years for molecular identifi-
368 cation and for structural elucidation [127–130]. COSY has been
369 employed in metabolomics research as it benefits from a relatively
370 short experimental time with the possibility of running a 2D spec-
371 trum in only a few minutes and providing far more information
372 than is gained from 1D NMR spectra. The simplest COSY pulse
373 sequence consists of a single 90° RF pulse followed by evolution
374 time (t_1) and then a second 90° pulse followed by a measurement
375 period (t_2). The COSY spectrum comprises a homonuclear, mostly
376 (^1H – ^1H), correlation spectrum in which the cross peaks in the 2D
377 spectrum indicate through bond couplings between pairs of nuclei.
378 The cross peaks represent through bond magnetization transfer
379 between two nuclei. This provides a powerful tool for the identifi-
380 cation of peaks that belong to the same molecule in samples com-
381 posed of many molecules, as would be the case for metabolites in
382 biological samples. As through bond correlation occurs only within
383 the same molecule, COSY NMR spectroscopy has been used in a
384 wide range of NMR-based metabolomics applications [131–135].
385 Figure 5 shows the 2D COSY NMR spectrum from which the cor-
386 relation between coupled protons can be used to assign an NMR
387 signal and to identify the corresponding molecule. However, for
388 multiple overlapped signals, 2D COSY is not powerful enough to
389 allow assignment of the individual signals. Other 2D NMR experi-
ments, such as total correlation spectroscopy (TOCSY), can be
used to assist with signal assignment.



this figure will be printed in b/w

Fig. 5 700 MHz 2D COSY NMR spectrum of *n*-butanol and *n*-propanol in CDCl_3

Total Correlation
Spectroscopy (TOCSY)

TOCSY or HOHAHA (Homonuclear Hartmann Hahn) is a similar approach to COSY, whereby the chemical shift of a given nucleus such as H is correlated with the chemical shift of other Hs of the same compound which are within the spin system (unbroken chain of couplings) of the atom. Similar to COSY, whereby the correlation between pairs of atoms (protons) in nearby carbon atoms that are connected by scalar coupling would be observed, the TOCSY spectrum shows the cross peaks not only for protons which are directly coupled but also for protons which are connected by a chain of couplings. For example, if proton A is coupled with proton B and proton B coupled with proton C, the COSY spectrum would express only the coupling A with B, whereas the TOCSY spectrum would display the coupling of A with both B and C. Figure 6 shows the stack plot of TOCSY (blue) and the COSY spectrum (red): more blue peaks can be observed, these representing every proton signal coupled with proton signals related to the same molecule (*n*-propanol and *n*-butanol). This shows that TOCSY spectrum can be used for resolving overlapped peaks that belong to different molecules. For instance, Fig. 7 shows an extended region of Fig. 6. Clearly, propanol peaks can be resolved from butanol peaks by simply detecting the signals that share four cross-correlation peaks (butanol, green arrow) compared with signals

390
391
392
393
394
395
396
397
398
399
400
401
402
403
404
405
406
407
408
409
410
411

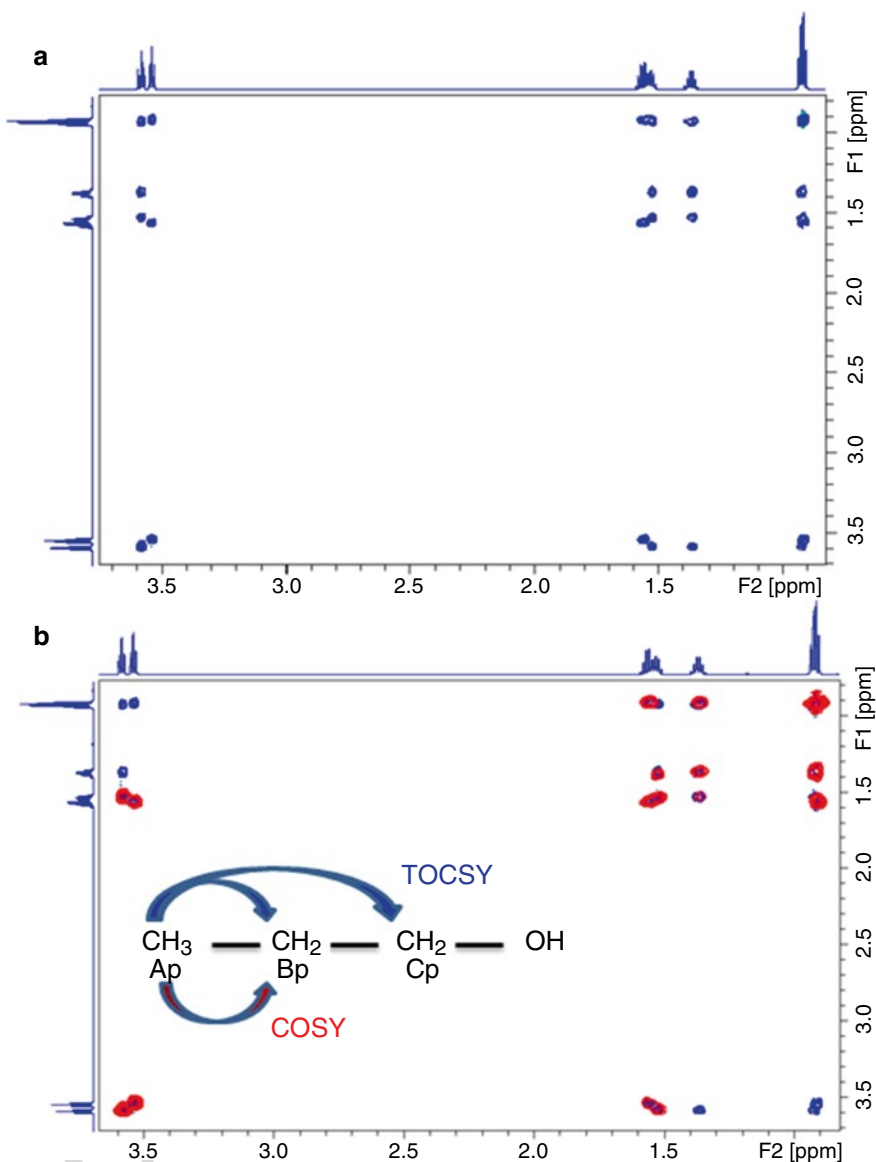
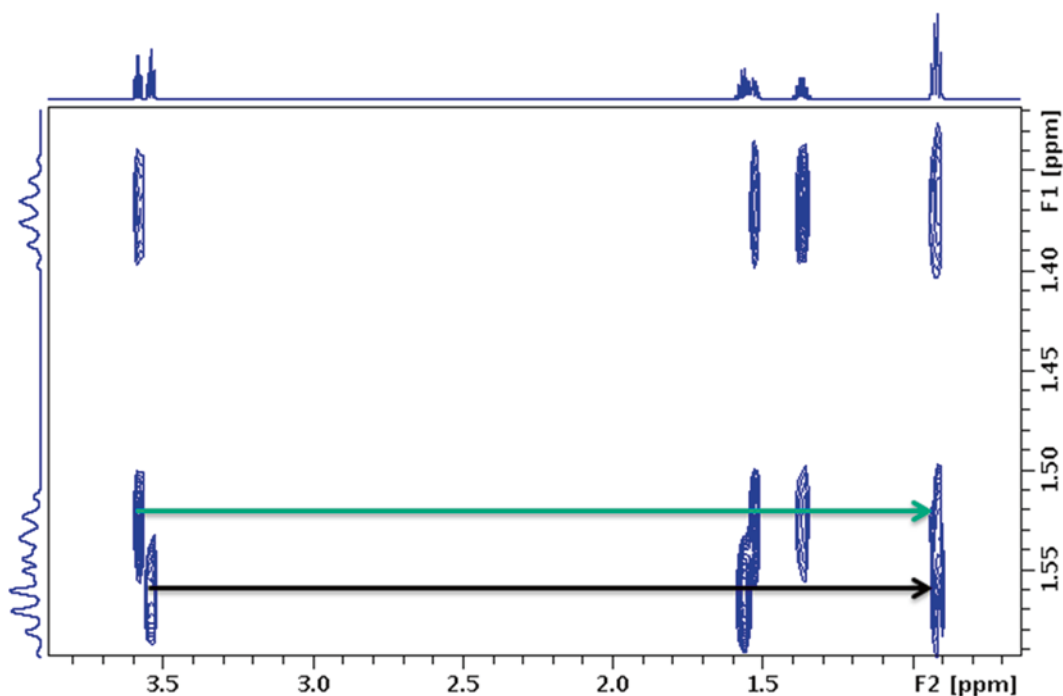


Fig. 6 (a) TOCSY NMR spectrum and (b) stack plot of TOCSY (*blue*) and COSY spectrum (*red*) for a mixed sample of *n*-propanol and *n*-butanol in CDCl_3 . A greater number of *blue* peaks (TOCSY) can be observed than COSY peaks (*red*). As anticipated, the COSY spectrum shows only the coupling between Ap and Bp, while the TOCSY spectrum displays the coupling of Ap with both Bp and Cp

412
413
414
415
416
417
418

that share only three cross peaks (propanol, black arrow). Assignment of peaks is accomplished by drawing a projection from the cross peak to 1D spectrum in the plot axis (Fig. 8). The arrow projection that connects the green arrow (butanol) with the signal at 3.584 ppm confirms that this peak refers to butanol, not propanol, and the second projection that correlates the signal at 1.564 ppm with the black arrow confirms that this peak corresponds to the



this figure will be printed in b/w

Fig. 7 Extended region of Fig. 6a

propanol molecule (Fig. 7). Confirmation of one peak as propanol and another peak as butanol would be sufficient to complete the assignment of all signals for both molecules using the TOCSY spectrum (Fig. 8). The assignment of ^1H NMR signals can be used in combination with other 2D NMR techniques, such as heteronuclear correlation spectroscopy. This will assist in the assignment of other nuclei signals such as those of the carbon NMR spectrum.

3.1.5 Heteronuclear Single-Quantum Correlation Spectroscopy (HSQC)

Bond correlation can also be used for correlation between two different types of nuclei (commonly ^1H with ^{13}C or ^{15}N), which are separated by one bond. For example, the ^1H - ^{13}C HSQC spectrum coordinates the chemical shift of protons and the corresponding bonded carbon, whereby only one cross peak will be obtained per pair of coupled atoms. Thus, HSQC offers a particularly informative approach for the assignment of signals, especially for the assignment of overlapping proton signals. Figure 9 shows the ^1H - ^{13}C HSQC of a mixture of *n*-butanol and *n*-propanol spectra in CDCl_3 . The figure demonstrates the efficacy of HSQC in resolving overlapped proton signals. For example, the extended region (A) resolved the overlapped proton signal at 0.91 ppm. Moreover, HSQC spectra can be used to assign both proton and carbon NMR spectra.

HSQC is also a useful technique to reduce the experimental time for nuclei with low sensitivity and low natural abundances,

419
420
421
422
423
424
425
426427
428
429
430
431
432
433
434
435
436
437
438
439
440
441

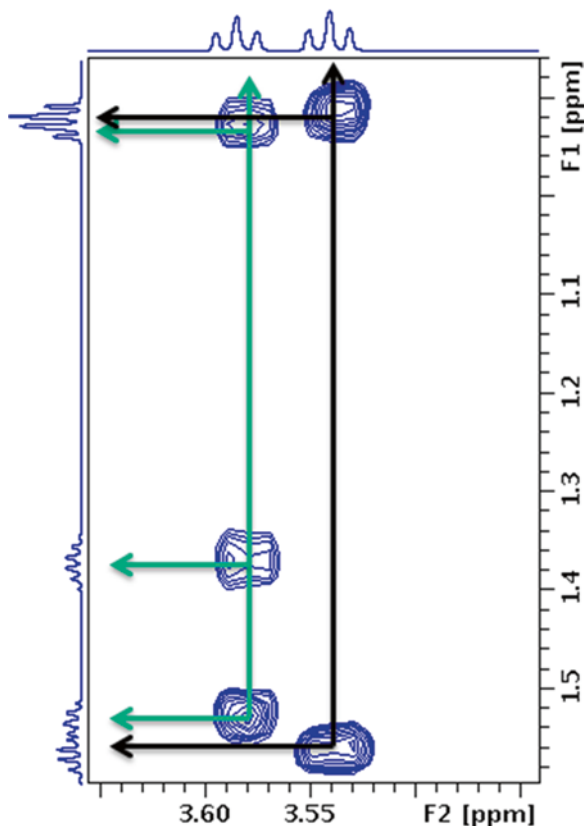
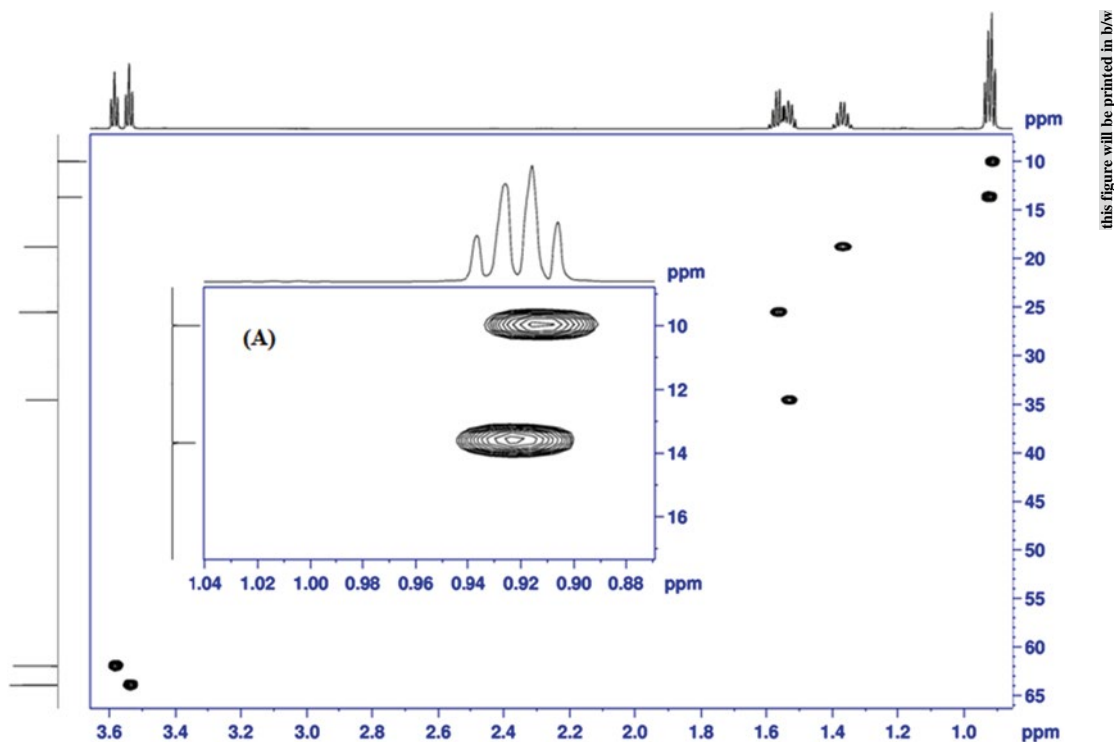


Fig. 8 Projection of the arrow that connects the *n*-butanol (green) and *n*-propanol (black) TOCSY cross peak with the corresponding 1D proton NMR spectrum

442
443
444
445
446
447
448
449
450
451
452
453
454
455
456
457
458
459
460

such as ^{13}C and ^{15}N , whereas the magnetization from the more sensitive nucleus I (usually ^1H) transferred to the less sensitive nucleus, such as ^{13}C and ^{15}N . ^1H - ^{15}N HSQC spectroscopy is one of the most important and common experimental techniques in the assignment of protein signals, as the assignment of NMR signals is the prerequisite step for the study of protein structure and dynamics [136–139]. Two-dimensional multiple-quantum correlation spectroscopy (HMQC) is a 2D heteronuclear correlation NMR approach similar to HSQC spectroscopy and provides identical information with a similar spectrum but uses different methods. Both HSQC and HMQC have been used in NMR-based metabolomics research, with HSQC being considered superior for larger molecules such as proteins [117, 133, 140].

HMBC (Heteronuclear Multiple Bond Correlation) is a 2D heteronuclear correlation technique that correlates the chemical shift of two different types of nuclei (i.e., ^{13}C and ^1H) that are separated from each other by two or more chemical bonds. The chemical shift of one nucleus, such as ^1H , is usually detected in the directly measured dimension (F2), and the chemical shift of the



this figure will be printed in b/w

Fig. 9 ^1H - ^{13}C HSQC spectrum of a mixture of *n*-butanol and *n*-propanol dissolved in CDCl_3 recorded using 700 MHz Bruker Avance (III) NMR spectrometer. The extended region (A) of the methyl group signals at 0.92 ppm indicates that this signal was resolved into two ^{13}C signals in the second dimension, one at 10 and the other at 13.85 ppm

other nucleus, such as ^{13}C (X-nucleus or heteronucleus), is recorded 461
 in the indirect dimension, as shown in Fig. 10. In this approach, a 462
 low-pass filtration is used to eliminate the single bond correlation 463
 known as “single-quantum coherence” corresponding with single 464
 bond interactions. For example, (^1H - ^{13}C) HMBC eliminates the 465
 single C-H bond correlation while correlating the chemical shift of 466
 H with C when separated by two or three bonds and, in some cases, 467
 with even more distant ones. Thus, (^1H - ^{13}C) HMBC is usually 468
 used for the assignment of signals of quaternary and carbonyl 469
 carbons. The combination of HMBC with HSQC or HMQC provides 470
 a powerful approach for assignment of signals. Figure 11 471
 shows both HMQC (red) and HMBC (blue), the seven red cross 472
 peaks being associated with the seven carbons in both *n*-propanol 473
 and *n*-butanol and the sixteen blue cross peaks being associated 474
 with the long bond correlation interactions. This figure demon- 475
 strates the power of combining and integrating the information 476
 from 2D NMR experiments for spectral assignment. The HMQC 477
 spectrum can be used to distinguish an overlapped signal from a 478
 separated one. For example, the proton multiplet signals observed 479
 around 0.92 ppm coupled with the two carbon peaks at 10.07 and 480

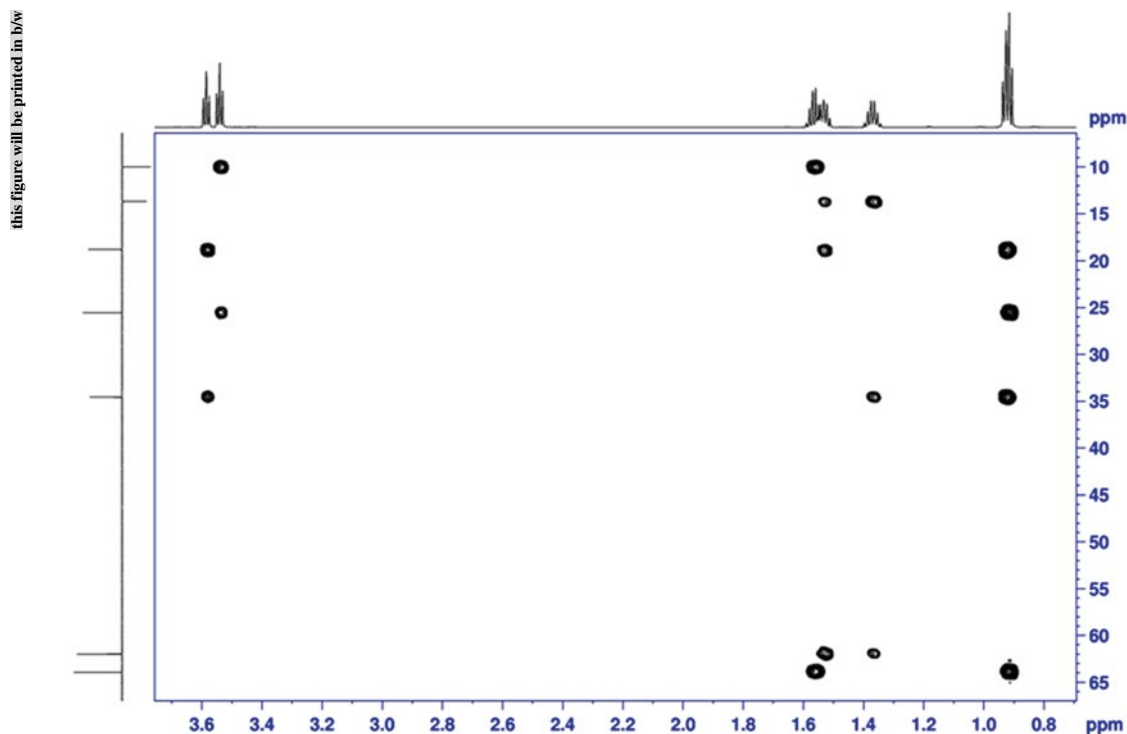


Fig. 10 ^{13}C - ^1H HSQC HMBC spectrum of a mixed sample composed of *n*-propanol and *n*-butanol in CDCl_3 . The long correlation between the 1D proton spectrum (*top* projection) and the ^{13}C DEPT-135 spectrum (*see* Fig. 4, *left* projection) is illustrated

481
482
483
484
485
486
487
488
489
490
491
492
493
494
495
496
497
498
499

13.79 ppm confirm that the proton NMR signal is indeed two overlapping ones. Similarly, the proton multiplet around 1.55 ppm is coupled with two carbon signals, while each one of the remaining proton signals at 1.37, 3.54, and 3.58 ppm is coupled with only one carbon signal. Moreover, HMBC and HSQC spectra can be used to separate and assign *n*-butanol peaks from *n*-propanol ones. For instance, the carbon HSQC cross peak (red) connecting the carbon signal at 25.67 ppm with proton resonance at 1.564 is aligned with two HMBC cross peaks (black arrows), so assigning the three peaks to the *n*-propanol molecule while the HSQC (red) aligned with three more blue HMBC cross peaks assigns these peaks to the *n*-butanol molecule (green arrows; *see* Fig. 12). Figure 13 demonstrates example models of chemical bond connections of *n*-butanol that can be studied by using 2D experiments for both homonuclear correlation and heteronuclear correlation. Details of the way in which these 2D experiments can be used to assign the proton and carbon NMR spectra of *n*-propanol and *n*-butanol are presented and the complete proton and carbon assignments provided in Table 2.

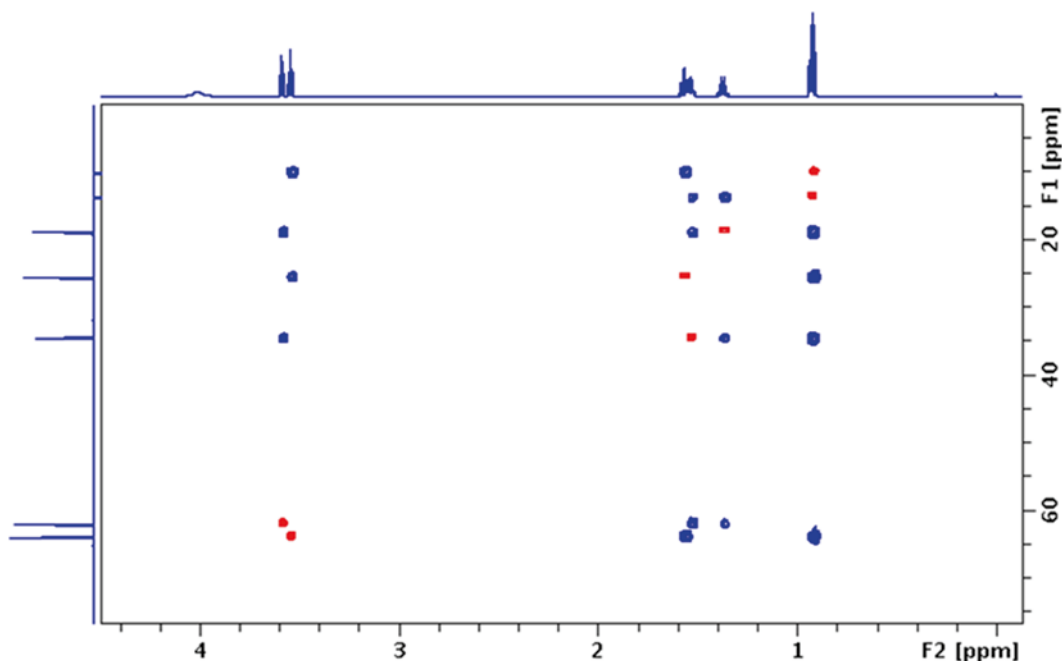


Fig. 11 Stack plot of ^{13}C - ^1H HSQC spectrum (*red*) and HMBC spectrum (*blue*) of a mixed sample of *n*-propanol and *n*-butanol in CDCl_3

3.2 Mass Spectrometry (MS)

Mass spectrometry (MS) is a powerful technique used mainly for the identification of unknown compounds and for the quantification of known molecules within a sample [71, 141–146]. As for NMR [28, 57, 147–152] and X-rays [153–160], it can also be used for structural elucidation and for study of the chemical properties of materials under investigation [161–166]. Due to its high sensitivity and selectivity, MS provides an important analytical platform for profiling metabolites in mixed samples, such as biological samples. Moreover, MS can detect ions that do not contain protons or carbon, such as metal ions. However, no MS method is perfect for the detection of all classes of metabolites, and so more than one method must be employed for comprehensive metabolic profiling. Figure 14 shows the main components of the MS instrument with the different sources of ionization and types of mass analyzer that can be used for the detection of different classes of molecule. The advantages of using GC-MS, for example, include high separation efficiency and reproducible retention times that may be exchanged between different laboratories for data comparison using the retention index concept with retention time as a marker [167]. However, the inherent limitation of GC-MS is the fact that it detects only volatile compounds or compounds that can be derivatized to become volatile. Furthermore, MS cannot detect all metabolites, as some metabolites do not ionize with certain

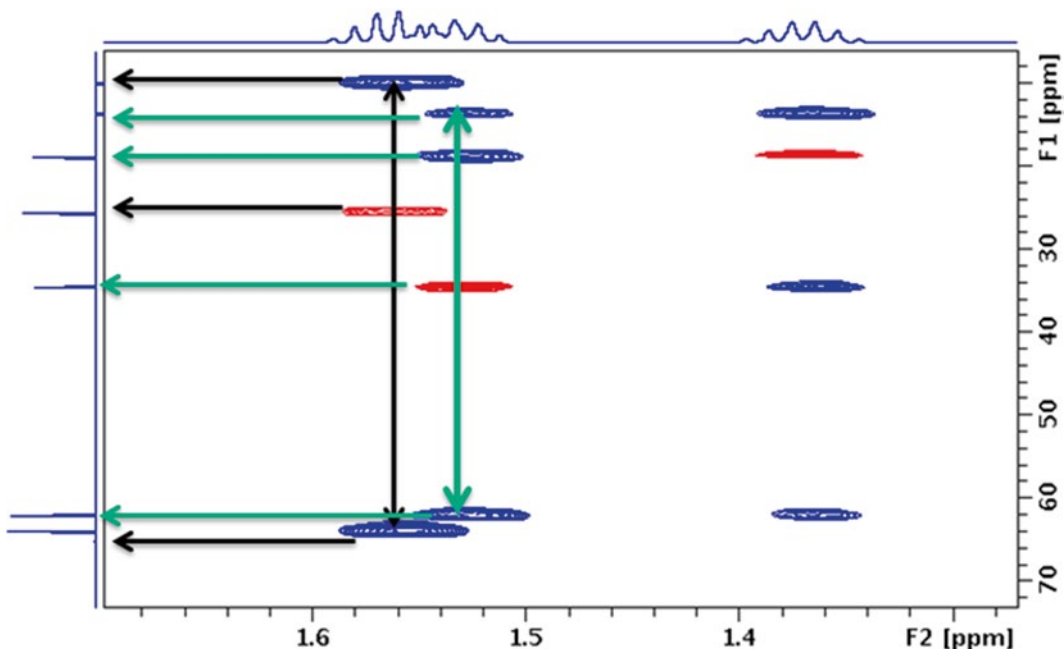


Fig. 12 Extended region of Fig. 11

this figure will be printed in b/w

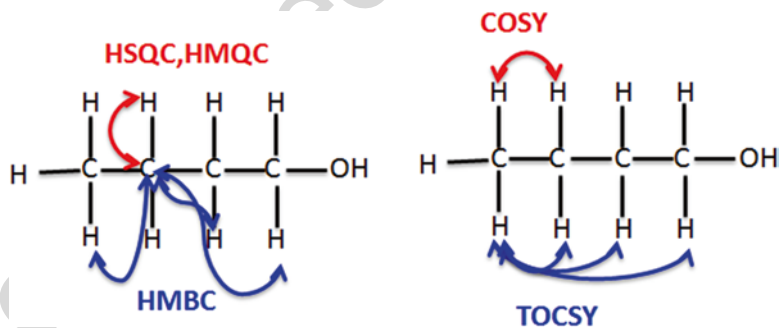


Fig. 13 The bond connection of *n*-butanol that can be studied by using different 2D NMR experiments for both a homonuclear correlation and a heteronuclear correlation

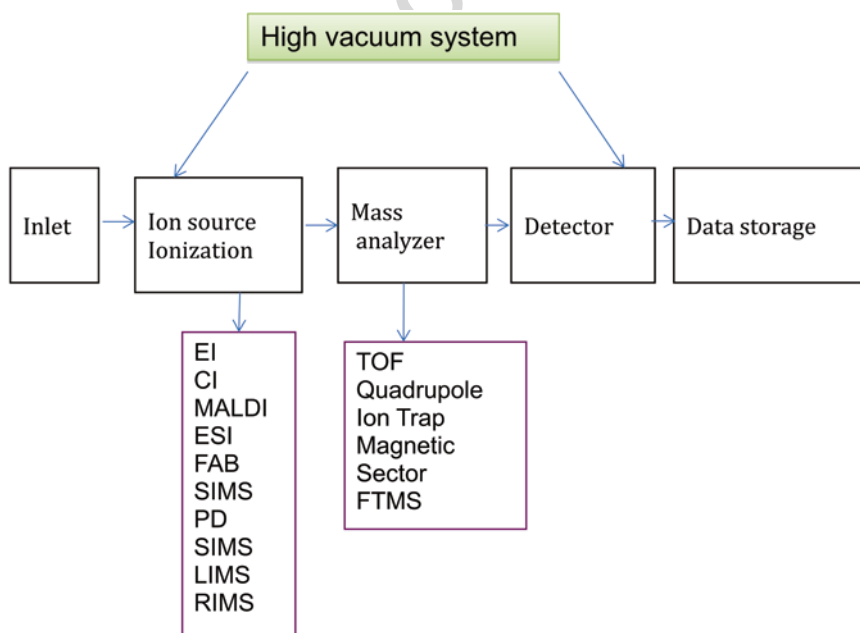
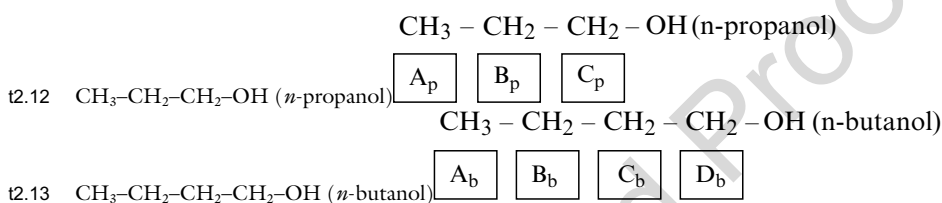
523
524
525
526
527
528
529
530
531
532
533

ionization methods. The dynamic range of the MS detector is still only three to four orders of magnitude, whereas the range of metabolite concentration is usually much larger, and no detector exists that can detect all metabolites. A general challenge in the metabolic proofing of biological samples is the fact that many metabolites have not yet been fully identified. For example, among the 869 different metabolites that have been detected in tomato, 494 are not found in the common metabolite databases [168].

The number and class of metabolites that can be detected by mass spectrometry depend on the choice of ionization mode. No single ionization method can cover all metabolite classes, such as

t2.1 **Table 2**
 t2.2 **Complete assignment of ^1H and ^{13}C NMR peaks for both *n*-propanol and *n*-butanol**
 t2.3 **using data from a number of 1D and 2D NMR experiments**

t2.4		Chemical shift of ^1H NMR signal ppm	Chemical shift of ^{13}C NMR signals ppm
t2.5	A_p	0.916	10.01
t2.6	A_b	0.926	13.79
t2.7	B_b	1.370	18.95
t2.8	C_b	1.533	34.56
t2.9	B_p	1.563	25.67
t2.10	C_p	3.539	64.05
t2.11	D_b	3.584	62.13



this figure will be printed in b/w

Fig. 14 Schematic plot of MS components including EI (electron impact), CI (chemical ionization), MALDI (matrix-assisted laser desorption ionization), ESI (electrospray ionization), FAB (fast-atom bombardment), SIMS (resonance ionization), PD (plasma-desorption ionization), LIMS (laser ionization), and RIMS (resonance ionization)

534 polar, nonpolar neutral, and ionic. Consequently, different ionization
535 methods should be used independently to maximize the number
536 of metabolites detected. For example, in LC-MS analysis, electro-
537 spray ionization (ESI) in positive mode is the most common
538 mode that can effectively ionize a wide range of medium-sized
539 polar molecules, whereas the negative ionization mode is more
540 powerful for certain metabolite classes, such as carbohydrates and
541 organic acids. For example, it was reported that use of both
542 atmospheric-pressure chemical ionization (APCI) and ESI
543 increased the coverage of the erythrocyte metabolome by 34 %.
544 It has been reported that by using a set of different complemen-
545 tary methods of GC-MS and LC-MS up to 100–500 metabolites
546 can be detected in a targeted analytical approach for blood sam-
547 ples, and about 600–1,000 can be detected in a fingerprinting
548 mode [169–171]. It is important to note that the strategy for
549 metabolite identification in LC-MS is different from that in
550 GC-MS, in which usually only the molecular ion is detected and
551 additional MS/MS experiments are required to gain information
552 about the identity and structure of the metabolites.

553 *3.2.1 Liquid*
554 *Chromatography–Mass*
555 *Spectrometry (LC-MS)*

556 LC-MS comprises two powerful analytical tools, high-performance
557 liquid chromatography (HPLC, known as high-pressure liquid
558 chromatography) and mass spectrometry. When combined,
559 LC-MS represents a very powerful analytical tool for the separa-
560 tion, identification, and quantification of molecules in a mixed
561 sample. The HPLC technique separates molecules first based on
562 different physical and chemical properties such as molecular size,
563 charge, polarity, and affinity toward other molecules. As for other
564 chromatography techniques, HPLC consists of a stationary phase
565 and a mobile phase. The stationary phase involves the use of mate-
566 rials such as silica gel that slow down the movement of molecules
567 to varying extents according to molecular size, so allowing separa-
568 tion of molecules based on size differences. The mobile phase
569 comprises the solution containing the sample mixture, and this
570 travels through the stationary phase (chromatography column)
571 where separation of molecules occurs. Column chromatography
572 can be used to purify individual chemical compounds from mix-
573 tures. Different samples require different columns, proteins, and
574 peptide samples, for example, requiring different columns from
575 those needed for samples of small molecules typical of metabolo-
576 mics studies. Once the analytes are separated, they pass through
577 the mass spectrometer analyzer where they are detected based on
578 the mass-to-charge ratio, and the intensity of each resultant line
579 corresponds to relative concentration of each molecule.

On the basis of its ability to separate and detect a wide range of
molecules, LC-MS is probably the most widely used mass spectrom-
etry technology, especially in the biosciences. LC-MS is a very adaptable

tool for carrying out the majority of metabolite profiling studies, allowing both quantitative and structural information to be obtained with high level of sensitivity. Different separation methods can be used to separate different classes of metabolite. For example, the reversed-phase (RP) gradient chromatography method has been the most commonly used separation method in LC-MS studies for global metabolite profiling [145, 172]. However, this is not the most appropriate method for polar and/or ionic species, which includes many important metabolites (organic acids or amino acids). These metabolites represent highly significant components in biochemical pathways, and their evaluation may be important in detecting critical metabolic states, such as inborn errors of metabolism and metabolic syndrome. Hydrophilic interaction chromatography (HILIC) is an alternative method that can be used to ionize polar metabolites, so increasing the breadth of metabolites detected [173]. In order to maximize the coverage of metabolites being profiled, the sample can be analyzed twice, either using RP and HILIC separately or using a column-switching approach of two-dimensional analysis in an “orthogonal” combination of HILIC and RP-LC [174–177]. Although the combined use of RP and HILIC is the preferable ionization method for many metabolites, this approach does not cover the whole range of metabolite polarities for biological samples such as urine [145]. Consequently, other ionization methods such as positive and negative electrospray ionization (ESI) modes and atmospheric-pressure chemical ionization (APCI) are recommended in order to maximize the breadth of detection of different metabolites in a biological sample [178]. Considering all these possibilities, analyses in eight different modes (eight separate runs) are required for comprehensive profiling of metabolites. These combinations widen the applications of LC-MS in metabolomics, and in fact, both targeted and nontargeted metabolomics analyses have increasingly been conducted using different methods of LC-MS [172, 179–188].

3.2.2 Gas Chromatography–Mass Spectrometry GC-MS

GC-MS is a novel tool for the analysis of volatile molecules, with a high-resolution and reproducible chromatographic separations due to the modern capillary GC, and these features render it well suited for the analysis of complex metabolic mixtures. As for LC-MS, GC-MS consists of two powerful analytical methods, gas chromatography and mass spectrometry. Together, these methods provide one of the most powerful methods of separation that can be used to provide qualitative and quantitative information about volatile compounds. The sample first goes through the gas chromatography unit where high-resolution separation of volatile organic compounds in a mixture is accomplished in the gas phase. The GC unit is composed mainly from columns, basically a tube which generally varies in length from less than 2 m up to 60 m or more, with a diameter ranging from 10 to 30 cm.

626
627
628
629
630
631
632
633
634
635
636
637
638
639
640
641
642
643
644
645
646
647
648
649
650
651
652
653
654
655
656
657
658
659
660
661
662
663
664
665
666
667
668
669
670
671
672

Different kinds of GC columns exist, such as packed and capillary tubes, which are designed to separate different kinds of samples. Packed tubes may be of stainless steel, glass, or fused silica and are usually formed as coils in order that they fit into an oven for high-temperature experiments, at around 250 °C. An inert gas, such as helium, is blown through the column; as the sample is inserted into the column, it becomes vaporized and the volatile molecules are pushed through the column by the helium. At the beginning, all the molecules move together but certain of them move slower than others, based on molecular weight and size. Smaller molecules travel faster than larger molecules, and as they progress through the column, the molecules continue to separate from each other and eventually emerge from the column as different components, so providing an effective approach to separation.

As the molecules exit the GC column, they are introduced into the MS unit where they are ionized using an ionization method such as an electron beam. The ions formed from a specific molecule will depend on the nature of that molecule, and both ionized molecules and ion fragments of the molecule are useable for distinguishing and identifying the components of a mixture at the molecular level based on the mass-to-charge ratio. Moreover, qualitative information about the components of a mixture can be obtained by measuring the absolute intensity of the peaks, where the highest peak is taken to represent 100 % abundance and used as reference for other peaks. Thus, GC-MS is the preferred analytical tool for the analysis of volatile metabolites and has been employed in different areas of metabolomics research including plant metabolomics and screening for inborn errors of metabolism [189–192]. In addition to well-established databases such as the Fiehn Metabolomics library, GC-MS provides good reproducibility and a highly reproducible fragmentation so offering a potent tool for the identification of metabolites. Other advantages include high sensitivity and resolution, low cost, and ease of use of instruments. The main limitation of GC-MS analysis is that it is limited to small volatile molecules, which means that this approach is of only limited application in global metabolic profiling studies. Moreover, the preparation of biological samples, such as bio-fluids, may be time-consuming and repetitive, this potentially leading to experimental error. Other problems such as product formation and degradation could occur during the ionization process. Moreover, during the derivatization reaction, nonvolatile metabolites could be converted into different forms of derivatives, leading to production of fragments, so that different forms of the same parent metabolite exist together. While analyzing real samples such as human urine which has a high variability in terms of metabolite content, derivatization may occur at different rates of conversion depending on the different properties of metabolites, so potentially

affecting reproducibility and overall results dramatically [193]. To overcome problems such as inaccurate quantification, a standard compound may be used for both derivatized standard compounds and for data correction processes, such as normalization.

To generate reproducible mass spectra and highly transferable EI-MS spectral libraries, use of standardized MS electron ionization energy of 70 eV is recommended to allow identification of compounds through mass spectral library matching, such as NIST and FiehnLib [194, 195].

Acknowledgments

We would like to thank *King Abdullah University of Science and Technology* for financial support and Dr. Virginia Unkefer and Dr. Zeyad Al Talla from KAUST and Dr. Christina Morris for their assistance and helpful editorial remarks.

[AU6] References

- 688 1. Al-Talla ZA, Akrawi SH, Tolley LT et al (2011) Bioequivalence assessment of two formulations of ibuprofen. *Drug Des Devel Ther* 5:427–433
- 689
- 690
- 691
- 692 2. Ibanez C, Simo C, Barupal DK et al (2013) A new metabolomic workflow for early detection of Alzheimer's disease. *J Chromatogr A* 1302:65–71
- 693
- 694
- 695
- 696 3. Wang X, Li K, Adams E et al (2013) Capillary electrophoresis-mass spectrometry in metabolomics: the potential for driving drug discovery and development. *Curr Drug Metab* 14:807–813
- 697
- 698
- 699
- 700
- 701 4. Zheng H, Clausen MR, Dalsgaard TK et al (2013) Time-saving design of experiment protocol for optimization of LC-MS data processing in metabolomic approaches. *Anal Chem* 85:7109–7116
- 702
- 703
- 704
- 705
- 706 5. Farag MA, Wessjohann LA (2012) Metabolome classification of commercial hypericum perforatum (St. John's Wort) preparations via UPLC-qTOF-MS and chemometrics. *Planta Med* 78:488–496
- 707
- 708
- 709
- 710
- 711 6. Wang B, Chen D, Chen Y et al (2012) Metabonomic profiles discriminate hepatocellular carcinoma from liver cirrhosis by ultraperformance liquid chromatography-mass spectrometry. *J Proteome Res* 11:1217–1227
- 712
- 713
- 714
- 715
- 716
- 717 7. Sun J, Von Tungeln LS, Hines W et al (2009) Identification of metabolite profiles of the catechol-O-methyl transferase inhibitor tolcapone in rat urine using LC/MS-based metabolomics analysis. *J Chromatogr B Analyt Technol Biomed Life Sci* 877:2557–2565
- 718
- 719
- 720
- 721
- 722
- 723 8. Wolfender J-L, Glauser G, Boccard J et al (2009) MS-based plant metabolomic approaches for biomarker discovery. *Nat Prod Commun* 4:1417–1430
- 724
- 725
- 726
- 727 9. Al-Talla ZA, Akrawi SH, Emwas AHM (2011) Solid state NMR and bioequivalence comparison of the pharmacokinetic parameters of two formulations of clindamycin. *Int J Clin Pharm Ther* 49:469–476
- 728
- 729
- 730
- 731
- 732 10. Ali K, Iqbal M, Yuliana ND et al (2013) Identification of bioactive metabolites against adenosine A1 receptor using NMR-based metabolomics. *Metabolomics* 9:778–785
- 733
- 734
- 735
- 736 11. Deja S, Barg E, Mlynarz P et al (2013) H-1 NMR-based metabolomics studies of urine reveal differences between type 1 diabetic patients with high and low HbA1c values. *J Pharm Biomed Anal* 83:43–48
- 737
- 738
- 739
- 740
- 741 12. Bu Q, Yan G, Deng P et al (2010) NMR-based metabonomic study of the sub-acute toxicity of titanium dioxide nanoparticles in rats after oral administration. *Nanotechnology* 21:1–12
- 742
- 743
- 744
- 745
- 746 13. Slupsky CM (2010) NMR-based analysis of metabolites in urine provides rapid diagnosis and etiology of pneumonia. *Biomark Med* 4:195–197
- 747
- 748
- 749

- 750 14. Emwas A-HMS, Salek RM, Griffin JL, 807
751 Merzaban J (2013) NMR-based metabolomics 808
752 in human disease diagnosis: applica- 809
753 tions, limitations, and recommendations. 810
754 *Metabolomics* 9:1048–1072 811
- 755 15. Sumner LW, Mendes P, Dixon RA (2003) 812
756 Plant metabolomics: large-scale phytochemis- 813
757 try in the functional genomics era. 814
758 *Phytochemistry* 62:817–836 815
- 759 16. Bedair M, Sumner LW (2008) Current and 816
760 emerging mass-spectrometry technologies 817
761 for metabolomics. *Trends Anal Chem* 27: 818
762 238–250 819
- 763 17. Connor SC, Wu W, Sweatman BC et al (2004) 820
764 Effects of feeding and body weight loss on the 821
765 1H-NMR-based urine metabolic profiles of 822
766 male Wistar Han rats: implications for bio- 823
767 marker discovery. *Biomarkers* 9:156–179 824
- 768 18. Morvan D, Demidem A, Papon J et al (2002) 825
769 Melanoma tumors acquire a new phospho- 826
770 lipid metabolism phenotype under cystemustine 827
771 as revealed by high-resolution magic 828
772 angle spinning proton nuclear magnetic reso- 829
773 nance spectroscopy of intact tumor sampled. 830
774 *Cancer Res* 62:1890–1897 831
- 775 19. Jimenez B, Mirnezami R, Kinross J et al (2013) 832
776 H-1 HR-MAS NMR spectroscopy of 833
777 tumor-induced local metabolic “field-effects” 834
778 enables colorectal cancer staging and prog- 835
779 nostication. *J Proteome Res* 12:959–968 836
- 780 20. Yang Y, Wang L, Wang S et al (2013) Study of 837
781 metabonomic profiles of human esophageal 838
782 carcinoma by use of high-resolution magic- 839
783 angle spinning H-1 NMR spectroscopy and 840
784 multivariate data analysis. *Anal Bioanal Chem* 841
785 405:3381–3389 842
- 786 21. DeFeo EM, Cheng LL (2010) Characterizing 843
787 human cancer metabolomics with ex vivo H-1 844
788 HRMAS MRS. *Technol Cancer Res Treat* 845
789 9:381–391 846
- 790 22. Moestue S, Sitter B, Bathen TF et al (2011) 847
791 HR MAS MR spectroscopy in metabolic char- 848
792 acterization of cancer. *Curr Top Med Chem* 849
793 11:2–26 850
- 794 23. Somashekar BS, Amin AG, Rithner CD et al (2011) 851
795 Metabolic profiling of lung granuloma 852
796 in mycobacterium tuberculosis infected guinea 853
797 pigs: ex vivo H-1 magic angle spinning NMR 854
798 studies. *J Proteome Res* 10:4186–4195 855
- 799 24. Somashekar BS, Kamarajan P, Danciu T et al (2011) 856
800 Magic angle spinning NMR-based 857
801 metabolic profiling of head and neck squa- 858
802 mous cell carcinoma tissues. *J Proteome Res* 859
803 10:5232–5241 860
- 804 25. Bouatra S, Aziat F, Mandal R et al (2013) 861
805 The human urine metabolome. *PLoS One* 862
806 8:e73076 863
26. Eddy MT, Belenky M, Sivertsen AC et al (2013) 807
(2013) Selectively dispersed isotope labeling 808
for protein structure determination by magic 809
angle spinning NMR. *J Biomol NMR* 57: 810
129–139 811
27. Koito Y, Yamada K, Ando S (2013) Solid- 812
state NMR and wide-angle X-ray diffraction 813
study of hydrofluoroether/beta-cyclodextrin 814
inclusion complex. *J Inclusion Phenom* 815
Macrocyclic Chem 76:143–150 816
28. Bouhrara M, Ranga C, Fihri A et al (2013) 817
Nitridated fibrous silica (KCC-1) as a sustain- 818
able solid base nanocatalyst. *ACS Sustainable* 819
Chem Eng 1:1192–1199 820
29. Jackson MD, Moon J, Gotti E et al (2013) 821
Material and elastic properties of 822
Al-tobermorite in ancient roman seawater 823
concrete. *J Am Ceram Soc* 96:2598–2606 824
30. Pettinari C, Caruso F, Zaffaroni N et al (2006) 825
Synthesis, spectroscopy (IR, multinu- 826
clear NMR, ESI-MS), diffraction, density 827
functional study and in vitro antiproliferative 828
activity of pyrazole-beta-diketone 829
dihalotin(IV) compounds on 5 melanoma cell 830
lines. *J Inorg Biochem* 100:58–69 831
31. Khan MT, Busch M, Molina VG et al (2014) 832
How different is the composition of the foul- 833
ing layer of wastewater reuse and seawater 834
desalination RO membranes? *Water Res* 59: 835
271–282 836
32. Hirano T, Nonoyama S, Miyajima T et al (1986) 837
Gas-phase F-19 and H-1 high- 838
resolution NMR-spectroscopy – application 839
to the study of unperturbed conformational 840
energies of 1,2-difluoroethane. *J Chem Soc* 841
Chem Commun 606–607 842
33. Marchione AA, Fagan PJ, Till EJ et al (2008) 843
Estimation of atmospheric lifetimes of hydro- 844
fluorocarbons, hydrofluoroethers, and olefins 845
by chlorine photolysis using gas-phase NMR 846
spectroscopy. *Anal Chem* 80:6317–6322 847
34. Krusic PJ, Shtarov AB, Roe DC et al (2010) 848
Chemical kinetics studied by gas-phase NMR 849
spectroscopy the encyclopedia of magnetic 850
resonance. Wiley, Hoboken, NJ, pp 233–250 851
35. Jackowski K (2006) Multinuclear NMR spec- 852
troscopy in the gas phase. *J Mol Struct* 853
786:215–219 854
36. Jackowski K (2001) Gas-phase O-17 and 855
S-33 NMR spectroscopy. *J Mol Struct* 563: 856
159–162 857
37. Widdifield CM, Bryce DL (2009) 858
Crystallographic structure refinement with 859
quadrupolar nuclei: a combined solid-state 860
NMR and GIPAW DFT example using 861
MgBr₂. *Phys Chem Chem Phys* 11: 862
7120–7122 863

- 864 38. Vyalikh A, Massiot D, Scheler U (2009) 921
865 Structural characterisation of aluminium lay- 922
866 ered double hydroxides by Al-27 solid-state 923
867 NMR. *Solid State Nucl Magn Reson* 924
868 36:19–23 925
- 869 39. Wiench JW, Avadhut YS, Maity N et al (2007) 926
870 Characterization of covalent linkages in 927
871 organically functionalized MCM-41 mesopo- 928
872 rous materials by solid-state NMR and theo- 929
873 retical calculations. *J Phys Chem B* 930
874 111:3877–3885 931
- 875 40. Ashbrook SE, Le Polles L, Pickard CJ et al 932
876 (2007) First-principles calculations of solid- 933
877 state O-17 and Si-29 NMR spectra of 934
878 Mg₂SiO₄ polymorphs. *Phys Chem Chem* 935
879 *Phys* 9:1587–1598 936
- 880 41. Shidong C, Maltsev S, Emwas AH et al 937
881 (2010) Solid-state NMR paramagnetic relax- 938
882 ation enhancement immersion depth studies 939
883 in phospholipid bilayers. *J Magn Reson* 207: 940
884 89–94 941
- 885 42. Patil U, Fihri A, Emwas A-H et al (2012) 942
886 Silicon oxynitrides of KCC-1, SBA-15 and 943
887 MCM-41 for CO₂ capture with excellent 944
888 stability and regenerability. *Chem Sci* 3: 945
889 2224–2229 946
- 890 43. Wong A, Li X, Sakellariou D (2013) Refined 947
891 magic-angle coil spinning resonator for nano- 948
892 liter NMR spectroscopy: enhanced spectral 949
893 resolution. *Anal Chem* 85:2021–2026 950
- 894 44. Tripathi P, Somashekar BS, Ponnusamy M 951
895 et al (2013) HR-MAS NMR tissue metabo- 952
896 lomic signatures cross-validated by mass 953
897 spectrometry distinguish bladder cancer 954
898 from benign disease. *J Proteome Res* 12: 955
899 3519–3528 956
- 900 45. Elbayed K, Berl V, Debeuckelaere C et al 957
901 (2013) HR-MAS NMR spectroscopy of 958
902 reconstructed human epidermis: potential for 959
903 the in situ investigation of the chemical inter- 960
904 actions between skin allergens and nucleo- 961
905 philic amino acids. *Chem Res Toxicol* 26: 962
906 136–145 963
- 907 46. Wilson M, Davies NP, Brundler M-A et al 964
908 (2009) High resolution magic angle spinning 965
909 ¹H NMR of childhood brain and nervous sys- 966
910 tem tumours. *Mol Cancer* 8:1–11 967
- 911 47. X-x G, W-y H, H-w Y et al (2008) Study of 968
912 malignant and normal tissues of the rectum 969
913 using NMR spectroscopy. *Guang Pu Xue Yu* 970
914 *Guang Pu Fen Xi* 28:2201–2206 971
- 915 48. De Silva SS, Payne GS, Thomas V et al (2009) 972
916 Investigation of metabolite changes in the 973
917 transition from pre-invasive to invasive cervi- 974
918 cal cancer measured using ¹H and ³¹P 975
919 magic angle spinning MRS of intact tissue. 976
920 *NMR Biomed* 22:191–198 977
49. Duarte IF, Stanley EG, Holmes E et al (2005) 921
Metabolic assessment of human liver trans- 922
plants from biopsy samples at the donor and 923
recipient stages using high-resolution magic 924
angle spinning ¹H NMR spectroscopy. *Anal* 925
Chem 77:5570–5578 926
50. Atiqullah M, Anantawaraskul S, Emwas 927
A-HM et al (2013) Effects of supported 928
((BuCp)-Bu-n)(²ZrCl₂) catalyst active-center 929
distribution on ethylene-1-hexene copolymer 930
backbone heterogeneity and thermal behav- 931
iors. *Ind Eng Chem Res* 52:9359–9373 932
51. Jackson MD, Chae SR, Mulcahy SR et al 933
(2013) Unlocking the secrets of 934
Al-tobermorite in Roman seawater concrete. 935
Am Mineral 98:1669–1687 936
52. Kamal MS, Bahuleyan BK, Sohail OB et al 937
(2013) Crystallization analysis fractionation of 938
poly(ethylene-co-styrene) produced by metal- 939
locene catalysts. *Polym Bull* 70:2645–2656 940
53. Abriata LA, Zaballa M-E, Berry RE et al 941
(2013) Electron spin density on the axial his 942
ligand of high-spin and low-spin nitrophorin 943
2 probed by heteronuclear NMR spectroscopy. 944
Inorg Chem 52:1285–1295 945
54. Kazansky LP, McGarvey BR (1999) NMR 946
and EPR spectroscopies and electron density 947
distribution in polyoxoanions. *Coord Chem* 948
Rev 188:157–210 949
55. Sereda GA, Borisenko AA, Lapteva VL et al 950
(1992) Study of substituents effect on the dis- 951
tribution of electron density in monosubstituted 952
and disubstituted triptycenes molecules 953
by the H-1 and C-13 NMR-spectroscopy. *Zh* 954
Org Khim 28:1105–1119 955
56. Tandura SN, Kolesnikov SP, Nosov KS et al 956
(1997) Electron density distributions in substi- 957
tuted 2,3,4,5-tetraphenyl-1-germacyclopenta- 958
2,4-dienes studied by NMR spectroscopy. *Russ* 959
Chem Bull 46:1859–1861 960
57. Atiqullah M, Winston MS, Bercaw JE et al 961
(2012) Effects of a vanadium post-metallocene 962
catalyst-induced polymer backbone inhomoge- 963
neity on UV oxidative degradation of the 964
resulting polyethylene film. *Polym Degrad* 965
Stab 97:1164–1177 966
58. Bahuleyan BK, De SK, Sarath PU et al (2012) 967
Effect of aluminium nitride on the properties 968
of polyethylene obtained by In situ polymer- 969
ization using Ni(II) diimine complex. 970
Macromol Res 20:772–775 971
59. Kirchheim AP, Dal Molin DC, Fischer P et al 972
(2011) Real-time high-resolution X-ray imag- 973
ing and nuclear magnetic resonance study of 974
the hydration of pure and Na-doped C(3)A in 975
the presence of sulfates. *Inorg Chem* 50: 976
1203–1212 977

- 978 60. Zhang B, Powers R (2012) Analysis of bacterial biofilms using NMR-based metabolomics. *Future Med Chem* 4:1273–1306 1035
- 979 61. Chaudhari SR, Mogurampelly S, Suryaprakash N (2013) Engagement of CF(3) group in N-H center dot center dot center dot F-C hydrogen bond in the solution state: NMR spectroscopy and MD simulation studies. *J Phys Chem B* 117:1123–1129 1036
- 980 62. Wang Q-Q, Day VW, Bowman-James K (2013) Chemistry and structure of a host-guest relationship: the power of NMR and X-ray diffraction in tandem. *J Am Chem Soc* 135:392–399 1037
- 981 63. Brown SP (2012) Applications of high-resolution H-1 solid-state NMR. *Solid State Nucl Magn Reson* 41:1–27 1038
- 982 64. Kinnun JJ, Leftin A, Brown MF (2013) Solid-state NMR spectroscopy for the physical chemistry laboratory. *J Chem Educ* 90:123–128 1039
- 983 65. Linenberger KJ, Emwas A-H, Peat I et al. (2009) Using NMR to determine the structure of a peptide: an inquiry approach for an upper level undergraduate laboratory. *Abstr Pap Am Chem Soc* 237 1040
- 984 66. Mroue KH, Emwas A-HM, Power WP (2010) Solid-state Al-27 nuclear magnetic resonance investigation of three aluminum-centered dyes. *Can J Chem* 88:111–123 1041
- 985 67. Oommen JM, Hussain MM, Emwas A-HM et al (2010) Nuclear magnetic resonance study of nanoscale ionic materials. *Electrochem Solid-State Lett* 13:K87–K88 1042
- 986 68. Shahid SA, Bardiaux B, Franks WT et al (2012) Membrane-protein structure determination by solid-state NMR spectroscopy of microcrystals. *Nat Meth* 9:1212–1217 1043
- 987 69. Zanzoni S, D'Onofrio M, Molinari H et al (2012) Recombinant proteins incorporating short non-native extensions may display increased aggregation propensity as detected by high resolution NMR spectroscopy. *Biochem Biophys Res Commun* 427:677–681 1044
- 988 70. Blindauer CA, Emwas AH, Holy A et al (1997) Complex formation of the antiviral 9-2-(phosphonomethoxy)ethyl adenine (PMEA) and of its N1, N3, and N7 deaza derivatives with copper(II) in aqueous solution. *Chem Eur J* 3:1526–1536 1045
- 989 71. Mattar SM, Emwas AH, Calhoun LA (2004) Spectroscopic studies of the intermediates in the conversion of 1,4,11,12-tetrahydro-9,10-anthraquinone to 9,10-anthraquinone by reaction with oxygen under basic conditions. *J Phys Chem A* 108:11545–11553 1046
- 990 72. Sahloul N, Emwas A, Power W et al (2005) Ethyl acrylate-hydroxyethyl acrylate and hydroxyethyl acrylate-methacrylic acid: reactivity ratio estimation from cross-linked polymer using high resolution magic angle spinning spectroscopy. *J Macromol Sci Pure Appl Chem* A42:1369–1385 1047
- 991 73. Subbarao YV, Ellis R, Paulsen GM et al (1977) Kinetics of pyropolyphosphate and tripolyphosphate hydrolyses in presence of corn and soybean roots as determined by NMR-spectroscopy. *Soil Sci Soc Am J* 41:316–318 1048
- 992 74. Wilson MA, Jones AJ, Williamson B (1978) Nuclear magnetic-resonance spectroscopy of humic materials. *Nature* 276:487–489 1049
- 993 75. Nageeb A, Al-Tawashi A, Mohammad Emwas A-H et al (2013) Comparison of artemisia annua bioactivities between traditional medicine and chemical extracts. *Curr Bioact Compd* 9:324–332 1050
- 994 76. Farshidfar F, Weljie AM, Kopciuk K et al (2012) Serum metabolomic profile as a means to distinguish stage of colorectal cancer. *Genome Med* 4:42 1051
- 995 77. Sachse D, Sletner L, Morkrid K et al (2012) Metabolic changes in urine during and after pregnancy in a large, multiethnic population-based cohort study of gestational diabetes. *PLoS One* 7:e52399 1052
- 996 78. Nahon P, Amathieu R, Triba MN et al (2012) Identification of serum proton NMR metabolomic fingerprints associated with hepatocellular carcinoma in patients with alcoholic cirrhosis. *Clin Cancer Res* 18:6714–6722 1053
- 997 79. Mehrpour M, Kyani A, Tafazzoli M et al (2013) A metabolomics investigation of multiple sclerosis by nuclear magnetic resonance. *Magn Reson Chem* 51:102–109 1054
- 998 80. Diaz SO, Barros AS, Goodfellow BJ et al (2013) Following healthy pregnancy by nuclear magnetic resonance (NMR) metabolic profiling of human urine. *J Proteome Res* 12:969–979 1055
- 999 81. Atzori L, Antonucci R, Barberini L et al (2010) ¹H NMR-based metabolic profiling of urine from children with nephrouropathies. *Front Biosci (Elite Ed)* 2:725–732 1056
- 1000 82. Culeddu N, Chessa M, Porcu MC et al (2012) NMR-based metabolomic study of type 1 diabetes. *Metabolomics* 8:1162–1169 1057
- 1001 83. Ala-Korpela M (2007) Potential role of body fluid H-1 NMR metabolomics as a prognostic and diagnostic tool. *Expert Rev Mol Diagn* 7:761–773 1058
- 1002 84. O'Connell TM (2012) Recent advances in metabolomics in oncology. *Bioanalysis* 4:431–451 1059
- 1003 1060
- 1004 1061
- 1005 1062
- 1006 1063
- 1007 1064
- 1008 1065
- 1009 1066
- 1010 1067
- 1011 1068
- 1012 1069
- 1013 1070
- 1014 1071
- 1015 1072
- 1016 1073
- 1017 1074
- 1018 1075
- 1019 1076
- 1020 1077
- 1021 1078
- 1022 1079
- 1023 1080
- 1024 1081
- 1025 1082
- 1026 1083
- 1027 1084
- 1028 1085
- 1029 1086
- 1030 1087
- 1031 1088
- 1032 1089
- 1033 1090
- 1034 1091

- 1092 85. Zhang J, Wei S, Liu L et al (2012) NMR-
1093 based metabolomics study of canine bladder
1094 cancer. *Biochim Biophys Acta*
1095 1822:1807–1814
- 1096 86. Nevedomskaya E, Pacchiarotta T, Artemov A
1097 et al (2012) H-1 NMR-based metabolic pro-
1098 filing of urinary tract infection: combining
1099 multiple statistical models and clinical data.
1100 *Metabolomics* 8:1227–1235
- 1101 87. Dong B, Jia J, Hu W et al (2013) Application
1102 of H-1 NMR metabonomics in predicting
1103 renal function recoverability after the relief of
1104 obstructive uropathy in adult patients. *Clin*
1105 *Biochem* 46:346–353
- 1106 88. Gruetter R, Weisdorf SA, Rajanayagan V et al
1107 (1998) Resolution improvements in in vivo
1108 H-1 NMR spectra with increased magnetic
1109 field strength. *J Magn Reson* 135:260–264
- 1110 89. Keun HC, Beckonert O, Griffin JL et al
1111 (2002) Cryogenic probe ¹³C NMR spectro-
1112 scopy of urine for metabonomic studies. *Anal*
1113 *Chem* 74:4588–4593
- 1114 90. Grimes JH, O'Connell TM (2011) The appli-
1115 cation of micro-coil NMR probe technology
1116 to metabolomics of urine and serum. *J Biomol*
1117 *NMR* 49:297–305
- 1118 91. Ardenkjær-Larsen JH, Fridlund B, Gram A
1119 et al (2003) Increase in signal-to-noise ratio
1120 of >10,000 times in liquid-state NMR. *Proc*
1121 *Natl Acad Sci* 100:10158–10163
- 1122 92. Day SE, Kettunen MI, Gallagher FA et al
1123 (2007) Detecting tumor response to treat-
1124 ment using hyperpolarized ¹³C magnetic
1125 resonance imaging and spectroscopy. *Nat*
1126 *Med* 13:1382–1387
- 1127 93. Emwas AH, Saunders M, Ludwig C et al
1128 (2008) Determinants for optimal enhance-
1129 ment in ex situ DNP experiments. *Appl Magn*
1130 *Reson* 34:483–494
- 1131 94. Chekmenev EY, Norton VA, Weitekamp DP
1132 et al (2009) Hyperpolarized ¹H NMR
1133 employing low γ nucleus for spin polarization
1134 storage. *J Am Chem Soc* 131:3164–3165
- 1135 95. Ludwig C, Marin-Montesinos I, Saunders
1136 MG et al (2010) Application of ex situ
1137 dynamic nuclear polarization in studying
1138 small molecules. *Phys Chem Chem Phys*
1139 12:5868–5871
- 1140 96. Garrod S, Humpfer E, Spraul M et al (1999)
1141 High-resolution magic angle spinning ¹H
1142 NMR spectroscopic studies on intact rat renal
1143 cortex and medulla. *Magn Reson Med*
1144 41:1108–1118
- 1145 97. Holmes E, Tsang TM, Tabrizi SJ (2006) The
1146 application of NMR-based metabonomics in
1147 neurological disorders. *NeuroRx* 3:358–372
98. Ratai EM, Pilkenton S, Lentz MR et al (2005) 1148
Comparisons of brain metabolites observed 1149
by HRMAS ¹H NMR of intact tissue and 1150
solution ¹H NMR of tissue extracts in SIV- 1151
infected macaques. *NMR Biomed* 18: 1152
242–251 1153
99. Griffin J, Walker L, Garrod S et al (2000) 1154
NMR spectroscopy based metabonomic stud- 1155
ies on the comparative biochemistry of the 1156
kidney and urine of the bank vole 1157
(*Clethrionomys glareolus*), wood mouse 1158
(*Apodemus sylvaticus*), white toothed shrew 1159
(*Crocidura suaveolens*) and the laboratory 1160
rat. *Comp Biochem Physiol B Biochem Mol* 1161
Biol 127:357–367 1162
100. Yang J, Xu G, Zheng Y et al (2004) Diagnosis 1163
of liver cancer using HPLC-based metabo- 1164
nomics avoiding false-positive result from 1165
hepatitis and hepatocirrhosis diseases. *J* 1166
Chromatogr B 813:59–65 1167
101. Griffin JL, Troke J, Walker LA et al (2000) 1168
The biochemical profile of rat testicular tissue 1169
as measured by magic angle spinning H-1 1170
NMR spectroscopy. *FEBS Lett* 486:225–229 1171
102. Monleon D, Morales JM, Gonzalez-Darder J 1172
et al (2008) Benign and atypical meningioma 1173
metabolic signatures by high-resolution 1174
magic-angle spinning molecular profiling. *J* 1175
Proteome Res 7:2882–2888 1176
103. Wang H, Wang L, Zhang H et al (2013) H-1 1177
NMR-based metabolic profiling of human 1178
rectal cancer tissue. *Mol Cancer* 12:121 1179
104. Kaplan O, van Zijl P, Cohen JS (1990) 1180
Information from combined ¹H and ³¹P 1181
NMR studies of cell extracts: differences in 1182
metabolism between drug-sensitive and drug- 1183
resistant MCF-7 human breast cancer cells. 1184
Biochem Biophys Res Commun 169: 1185
383–390 1186
105. Ruiz-Cabello J, Cohen JS (1992) 1187
Phospholipid metabolites as indicators of can- 1188
cer cell function. *NMR Biomed* 5:226–233 1189
106. Emwas AHM, Al-Talla ZA, Guo XR et al 1190
(2013) Utilizing NMR and EPR spectro- 1191
scopy to probe the role of copper in prion dis- 1192
eases. *Magn Reson Chem* 51:255–268 1193
107. Kamal MZ, Yedavalli P, Deshmukh MV et al 1194
(2013) Lipase in aqueous-polar organic sol- 1195
vents: activity, structure, and stability. *Protein* 1196
Sci 22:904–915 1197
108. Samal RP, Khedkar VM, Pissurlenkar RRS 1198
et al (2013) Design, synthesis, structural char- 1199
acterization by IR, ¹H, ¹³C, ¹⁵N, 2D-NMR, 1200
X-ray diffraction and evaluation of a new class 1201
of phenylaminoacetic acid benzylidene hydra- 1202
zines as pFENR inhibitors. *Chem Biol Drug* 1203
Des 81:715–729 1204

- 1205 109. Cho BP, Kadlubar FF, Culp SJ et al (1990) 1262
 1206 N-15 nuclear-magnetic-resonance studies on 1263
 1207 the tautomerism of 8-hydroxy-2'- 1264
 1208 deoxyguanosine, 8-hydroxyguanosine, and 1265
 1209 other C8-substituted guanine nucleosides. 1266
 1210 Chem Res Toxicol 3:445–452
- 1211 110. Gronenborn AM, Wingfield PT, Clore GM 1267
 1212 (1989) Determination of the secondary struc- 1268
 1213 ture of the DNA-binding protein Ner from 1269
 1214 phage Mu using H-1 homonuclear and 1270
 1215 N-15-H-1 heteronuclear NMR-spectroscopy. 1271
 1216 Biochemistry 28:5081–5089
- 1217 111. Liu S, Howell M, Melby J et al (2012) H-1, 1272
 1218 C-13 and N-15 resonance assignment of the 1273
 1219 anticodon binding domain of human lysyl 1274
 1220 aminoacyl tRNA synthetase. Biomol NMR 1275
 1221 Assign 6:173–176 1276
- 1222 112. Martino L, Conte MR (2012) Biosynthetic 1277
 1223 preparation of ¹³C/¹⁵N-labeled rNTPs for 1278
 1224 high-resolution NMR studies of RNAs. 1279
 1225 Methods Mol Biol 941:227–245 1280
- 1226 113. Xi Y, de Ropp JS, Viant MR et al (2006) 1281
 1227 Automated screening for metabolites in com- 1282
 1228 plex mixtures using 2D COSY NMR spec- 1283
 1229 troscopy. Metabolomics 2:221–233 1284
- 1230 114. Sandusky P, Rafferty D (2005) Use of selective 1285
 1231 TOCSY NMR experiments for quantifying 1286
 1232 minor components in complex mixtures: 1287
 1233 application to the metabolomics of amino 1288
 1234 acids in honey. Anal Chem 77:2455–2463 1289
- 1235 115. Beckonert O, Keun HC, Ebbels TMD et al 1290
 1236 (2007) Metabolic profiling, metabolomic and 1291
 1237 metabolomic procedures for NMR spectro- 1292
 1238 scopy of urine, plasma, serum and tissue 1293
 1239 extracts. Nat Protoc 2:2692–2703 1294
- 1240 116. Nicholson JK, Foxall PJD, Spraul M et al 1295
 1241 (1995) 750 MHz ¹H and ¹H-¹³C NMR 1296
 1242 spectroscopy of human blood plasma. Anal 1297
 1243 Chem 67:793–811 1298
- 1244 117. Yuk J, McKelvie JR, Simpson MJ et al (2010) 1299
 1245 Comparison of 1-D and 2-D NMR tech- 1300
 1246 niques for screening earthworm responses to 1301
 1247 sub-lethal endosulfan exposure. Environ 1302
 1248 Chem 7:524–536 1303
- 1249 118. Ludwig C, Ward DG, Martin A et al (2009) 1304
 1250 Fast targeted multidimensional NMR metab- 1305
 1251 olomics of colorectal cancer. Magn Reson 1306
 1252 Chem 47:S68–S73 1307
- 1253 119. Xia J, Bjorndahl TC, Tang P et al (2008) 1308
 1254 MetaboMiner – semi-automated identifica- 1309
 1255 tion of metabolites from 2D NMR spectra of 1310
 1256 complex biofluids. BMC Bioinformatics 9 1311
- 1257 120. Fonville JM, Maher AD, Coen M et al (2010) 1312
 1258 Evaluation of full-resolution J-resolved ¹H 1313
 1259 NMR projections of biofluids for metabo- 1314
 1260 nomics information retrieval and biomarker 1315
 1261 identification. Anal Chem 82:1811–1821 1316
121. Mannina L, Sobolev A, Capitani D et al 1317
 (2008) NMR metabolic profiling of organic 1318
 and aqueous sea bass extracts: implications in 1319
 the discrimination of wild and cultured sea 1320
 bass. Talanta 77:433–444 1321
122. Griffin JL, Williams HJ, Sang E et al (2001) 1322
 Abnormal lipid profile of dystrophic cardiac 1323
 tissue as demonstrated by one- and two- 1324
 dimensional magic-angle spinning H-1 NMR 1325
 spectroscopy. Magn Reson Med 46:249–255 1326
123. Hyberts SG, Heffron GJ, Tarragona NG et al 1327
 (2007) Ultrahigh-resolution ¹H-¹³C HSQC 1328
 spectra of metabolite mixtures using nonlin- 1329
 ear sampling and forward maximum entropy 1330
 reconstruction. J Am Chem Soc 1331
 129:5108–5116 1332
124. Tang H, Wang Y, Nicholson JK et al (2004) 1333
 Use of relaxation-edited one-dimensional and 1334
 two dimensional nuclear magnetic resonance 1335
 spectroscopy to improve detection of small 1336
 metabolites in blood plasma. Anal Biochem 1337
 325:260–272 1338
125. Dumas ME, Canlet C, Vercauteren J et al 1339
 (2005) Homeostatic signature of anabolic 1340
 steroids in cattle using ¹H-¹³C HMBC NMR 1341
 metabolomics. J Proteome Res 1342
 4:1493–1502 1343
126. Dumas ME, Canlet C, André F et al (2002) 1344
 Metabonomic assessment of physiological dis- 1345
 ruptions using ¹H-¹³C HMBC-NMR spec- 1346
 troscopy combined with pattern recognition 1347
 procedures performed on filtered variables. 1348
 Anal Chem 74:2261–2273 1349
127. Kono H (2013) (¹H) and (¹³C) chemical 1350
 shift assignment of the monomers that com- 1351
 prise carboxymethyl cellulose. Carbohydr 1352
 Polym 97:384–390 1353
128. Hunt CT, Boulanger Y, Fesik SW et al (1984) 1354
 NMR analysis of the structure and metal 1355
 sequestering properties of metallothioneins. 1356
 Environ Health Perspect 54:135–145 1357
129. Lown JW, Hanstock CC (1985) High-field 1358
¹H-NMR analysis of the 1-1 intercalation 1359
 complex of the antitumor agent mitoxantrone 1360
 and the DNA duplex D(Cpgpcpg) 2. J Biomol 1361
 Struct Dyn 2:1097–1106 1362
130. Macura S, Kumar NG, Brown LR (1983) 1363
 Combined use of cosy and double quantum 1364
 two-dimensional NMR-spectroscopy for elu- 1365
 cidation of spin systems in polymyxin-B. 1366
 Biochem Biophys Res Commun 117:486–492 1367
131. Kim HK, Choi YH, Verpoorte R (2010) 1368
 NMR-based metabolomic analysis of plants. 1369
 Nat Protoc 5:536–549 1370
132. Le Guennec A, Tea I, Antheaume I et al 1371
 (2012) Fast determination of absolute metab- 1372
 olite concentrations by spatially encoded 2D 1373

- 1319 NMR: application to breast cancer cell
1320 extracts. *Anal Chem* 84:10831–10837
- 1321 133. Sekiyama Y, Chikayama E, Kikuchi J (2011)
1322 Evaluation of a semipolar solvent system as a
1323 step toward heteronuclear multidimensional
1324 NMR-based metabolomics for C-13-labelled
1325 bacteria, plants, and animals. *Anal Chem*
1326 83:719–726
- 1327 134. Flores-Sanchez IJ, Choi YH, Verpoorte R
1328 (2012) Metabolite analysis of *Cannabis sativa*
1329 L. by NMR spectroscopy. In: Kaufmann M,
1330 Klinger C (eds) *Functional genomics: meth-*
1331 *ods and protocols*, vol 815, 2nd edn, *Methods*
1332 *Mol Biol.*, pp 363–375
- 1333 135. Blasco H, Corcia P, Moreau C et al (2010)
1334 1H-NMR-based metabolomic profiling of
1335 CSF in early amyotrophic lateral sclerosis.
1336 *PLoS One* 5:e13223
- 1337 136. Yi Q, Scalley-Kim ML, Alm EJ et al (2000)
1338 NMR characterization of residual structure in
1339 the denatured state of protein L. *J Mol Biol*
1340 299:1341–1351
- 1341 137. Lee S-H, Cha E-J, Lim J-E et al (2012)
1342 Structural characterization of an intrinsically
1343 unfolded mini-HBX protein from hepatitis B
1344 virus. *Mol Cells* 34:165–169
- 1345 138. Robertson IM, Boyko RF, Sykes BD (2011)
1346 Visualizing the principal component of H-1,
1347 N-15-HSQC NMR spectral changes that
1348 reflect protein structural or functional proper-
1349 ties: application to troponin C. *J Biomol*
1350 *NMR* 51:115–122
- 1351 139. Liu H-K, Parkinson JA, Bella J et al (2010)
1352 Penetrative DNA intercalation and G-base
1353 selectivity of an organometallic tetrahydroan-
1354 thracene Ru-II anticancer complex. *Chem Sci*
1355 1:258–270
- 1356 140. Xi Y, de Ropp JS, Viant MR et al (2008)
1357 Improved identification of metabolites in
1358 complex mixtures using HSQC NMR spec-
1359 troscopy. *Anal Chim Acta* 614:127–133
- 1360 141. Raji M, Amad M, Emwas AH (2013)
1361 Dehydrodimerization of pterostilbene during
1362 electrospray ionization mass spectrometry.
1363 *Rapid Commun Mass Spectrom* 27:
1364 1260–1266
- 1365 142. Burton L, Ivosev G, Tate S et al (2008)
1366 Instrumental and experimental effects in
1367 LC-MS-based metabolomics. *J Chromatogr*
1368 *B Anal Technol Biomed Life Sci* 871:
1369 227–235
- 1370 143. Chen Y, Zhang R, Song Y et al (2009)
1371 RRLC-MS/MS-based metabolomics com-
1372 bined with in-depth analysis of metabolic
1373 correlation network: finding potential bio-
1374 markers for breast cancer. *Analyst* 134:
1375 2003–2011
144. Michopoulos F, Lai L, Gika H et al (2009) 1376
UPLC-MS-based analysis of human plasma 1377
for metabolomics using solvent precipitation 1378
or solid phase extraction. *J Proteome Res* 1379
8:2114–2121 1380
145. Theodoridis G, Gika HG, Wilson ID (2008) 1381
LC-MS-based methodology for global metab- 1382
olite profiling in metabolomics/metabolomics. 1383
Trends Anal Chem 27:251–260 1384
146. Waybright TJ, Van QN, Muschik GM et al 1385
(2006) LC-MS in metabolomics: optimiza- 1386
tion of experimental conditions for the analy- 1387
sis of metabolites in human urine. *J Liq* 1388
Chromatogr Relat Technol 29:2475–2497 1389
147. Allix M, Alba MD, Florian P et al (2011) 1390
Structural elucidation of beta-(Y, Sc)(2)Si2O7: 1391
combined use of Y-89 MAS NMR and powder 1392
diffraction. *J Appl Crystallogr* 44:846–852 1393
148. Singhal A (2009) Structural aspects of zeo- 1394
lites and oxide glasses: insights from solid 1395
state nuclear magnetic resonance. *Mater Sci* 1396
Found 49–51:149–192 1397
149. Das SK, Xu S, Emwas A-H et al (2012) High 1398
energy lithium-oxygen batteries – transport 1399
barriers and thermodynamics. *Energy Environ* 1400
Sci 5:8927–8931 1401
150. Loquet A, Habenstein B, Lange A (2013) 1402
Structural investigations of molecular 1403
machines by solid-state NMR. *Acc Chem Res* 1404
46:2070–2079 1405
151. Rouge P, Cornu A, Biesse-Martin A-S et al 1406
(2013) Identification of quinoline, carboline 1407
and glycinamide compounds in cow milk 1408
using HRMS and NMR. *Food Chem* 1409
141:1888–1894 1410
152. Weingarth M, Baldus M (2013) Solid-state 1411
NMR-based approaches for supramolecular 1412
structure elucidation. *Acc Chem Res* 46:
1413 2037–2046 1414
153. Barbul I, Varga RA, Silvestru C (2013) 1415
Structural diversity of coordination cores in 1416
homoleptic tetraaryltin(IV) dioxolane, alde- 1417
hyde and imines: the first octacoordinated 1418
double helicate tetraorganotin(IV) com- 1419
pound. *Eur J Inorg Chem* 18:3146–3154 1420
154. Ghazzali M, El-Faham A, Abdel-Megeed A 1421
et al (2012) Microwave-assisted synthesis, 1422
structural elucidation and biological assess- 1423
ment of 2-(2-(acetamidophenyl)-2-oxo-N 1424
phenyl acetamide and N-(2-(2-oxo- 1425
2-(phenylamino)acetyl)phenyl)propionamide 1426
derivatives. *J Mol Struct* 1013:163–167 1427
155. Niemyjska M, Maciejewska D, Wolska I et al 1428
(2012) Synthesis, structural investigations, 1429
and anti-cancer activity of new methyl indole- 1430
3-carboxylate derivatives. *J Mol Struct* 1026:
1431 30–35 1432

- 1433 156. Uma Devi T, Priya S, Selvanayagam S et al
1434 (2012) Synthesis, structural elucidation
1435 and spectroscopic analysis of 3a,8b-dihydroxy-
1436 4-oxo-1H,2H,3H,3aH,4H,8bH-indeno
1437 1,2-d imidazolidin-2-iminium chloride.
1438 Spectrochim Acta A Mol Biomol Spectrosc
1439 97:1063–1071
- 1440 157. Abuhijleh AL, Abu Ali H, Emwas A-H (2009)
1441 Synthesis, spectral and structural characteriza-
1442 tion of dinuclear rhodium (II) complexes of
1443 the anticonvulsant drug valproate with the-
1444 ophylline and caffeine. J Organomet Chem
1445 694:3590–3596
- 1446 158. Tegoni M, Ferretti L, Sansone F et al (2007)
1447 Synthesis, solution thermodynamics, and
1448 X-ray study of Cu-II 12 metallacrown-4 with
1449 GABA hydroxamic acid: an unprecedented
1450 crystal structure of a 12 MC-4 with a
1451 gamma-aminohydroxamate. Chemistry 13:
1452 1300–1308
- 1453 159. Al-Masri HT, Emwas A-HM, Al-Talla ZA
1454 et al (2012) Synthesis and characterization of
1455 new N-(diphenylphosphino)-naphthylamine
1456 chalcogenides: X-ray structures of
1457 (1-Nhcl10h7)P(Se)Ph-2 And Ph2p(S)Op(S)
1458 Ph-2. Phosphorus Sulfur Silicon Relat Elem
1459 187:1082–1090
- 1460 160. Decken A, Mattar SM, Emwas A (2005)
1461 1,4,11,12-Tetrahydro-9,10-anthraquinone.
1462 Acta Crystallogr Sect E Struct Rep Online
1463 61:O641–O642
- 1464 161. Reepmeyer JC, Woodruff JT, d'Avignon DA
1465 (2007) Structure elucidation of a novel ana-
1466 logue of sildenafil detected as an adulterant in
1467 an herbal dietary supplement. J Pharm
1468 Biomed Anal 43:1615–1621
- 1469 162. Riddell N, Arsenaault G, Klein J et al (2009)
1470 Structural characterization and thermal stabi-
1471 lities of the isomers of the brominated flame
1472 retardant 1,2,5,6-tetrabromocyclooctane
1473 (TBCO). Chemosphere 74:1538–1543
- 1474 163. Wu C, Chen F, Wang X et al (2007)
1475 Identification of antioxidant phenolic com-
1476 pounds in feverfew (*Tanacetum parthenium*)
1477 by HPLC-ESI-MS/MS and NMR. Phytochem
1478 Anal 18:401–410
- 1479 164. Zhou A, Kikandi S, Sadik OA (2007)
1480 Electrochemical degradation of quercetin:
1481 isolation and structural elucidation of the
1482 degradation products. Electrochem Commun
1483 9:2246–2255
- 1484 165. Bretz M, Gockler S, Humpf HU (2005)
1485 Isolation and structural elucidation of thermal
1486 degradation products of the *Fusarium* myco-
1487 toxin nivalenol. Mycotoxin Res 21:15–17
- 1488 166. Wolff JC, Hawtin PN, Monte S et al (2001)
1489 The use of particle beam mass spectrometry
for the measurement of impurities in a nabum-
etone drug substance, not easily amenable to
atmospheric pressure ionisation techniques.
Rapid Commun Mass Spectrom 15:265–272
167. Scalbert A, Brennan L, Fiehn O et al (2009)
Mass-spectrometry-based metabolomics: lim-
itations and recommendations for future
progress with particular focus on nutrition
research. Metabolomics 5:435–458
168. Iijima Y, Nakamura Y, Ogata Y et al (2008)
Metabolite annotations based on the integra-
tion of mass spectral information. Plant J
54:949–962
169. Lawton KA, Berger A, Mitchell M et al
(2008) Analysis of the adult human plasma
metabolome. Pharmacogenomics 9:383–397
170. A J, Trygg J, Gullberg J et al (2005) Extraction
and GC/MS analysis of the human blood
plasma metabolome. Anal Chem 77:
8086–8094
171. Shaham O, Wei R, Wang TJ et al (2008)
Metabolic profiling of the human response to
a glucose challenge reveals distinct axes of
insulin sensitivity. Mol Syst Biol 4:214
172. Theodoridis GA, Gika HG, Want EJ et al
(2012) Liquid chromatography-mass spec-
trometry based global metabolite profiling: a
review. Anal Chim Acta 711:7–16
173. Masson P, Alves AC, Ebbels TMD et al
(2010) Optimization and evaluation of
metabolite extraction protocols for untar-
geted metabolic profiling of liver samples by
UPLC-MS. Anal Chem 82:7779–7786
174. Gika HG, Theodoridis GA, Wilson ID (2008)
Hydrophilic interaction and reversed-phase
ultra-performance liquid chromatography
TOF-MS for metabolomic analysis of Zucker
rat urine. J Sep Sci 31:1598–1608
175. Spagou K, Tsoukali H, Raikos N et al (2010)
Hydrophilic interaction chromatography cou-
pled to MS for metabolomic/metabolomic
studies. J Sep Sci 33:716–727
176. Spagou K, Wilson ID, Masson P et al (2011)
HILIC-UPLC-MS for exploratory urinary
metabolic profiling in toxicological studies.
Anal Chem 83:382–390
177. Wang Y, Lehmann R, Lu X et al (2008)
Novel, fully automatic hydrophilic interac-
tion/reversed-phase column-switching high-
performance liquid chromatographic system
for the complementary analysis of polar and
apolar compounds in complex samples. J
Chromatogr A 1204:28–34
178. Sana TR, Waddell K, Fischer SM (2008) A
sample extraction and chromatographic strat-
egy for increasing LC/MS detection coverage

- 1546 of the erythrocyte metabolome. *J Chromatogr*
 1547 *B Analyt Technol Biomed Life Sci* 871:
 1548 314–321
- 1549 179. Lu W, Bennett BD, Rabinowitz JD (2008)
 1550 Analytical strategies for LC-MS-based tar-
 1551 geted metabolomics. *J Chromatogr B Analyt*
 1552 *Technol Biomed Life Sci* 871:236–242
- 1553 180. Yao W, He M, Jiang Y et al (2013) Integrated
 1554 LC/MS and GC/MS metabolomics data for
 1555 the evaluation of protection function of fruc-
 1556 tus *ligustri lucidi* on mouse liver.
 1557 *Chromatographia* 76:1171–1179
- 1558 181. Lee D-K, Yoon MH, Kang YP et al (2013)
 1559 Comparison of primary and secondary metab-
 1560 olites for suitability to discriminate the origins
 1561 of *Schisandra chinensis* by GC/MS and LC/
 1562 MS. *Food Chem* 141:3931–3937
- 1563 182. Guo B, Chen B, Liu A et al (2012) Liquid
 1564 chromatography-mass spectrometric multiple
 1565 reaction monitoring-based strategies for
 1566 expanding targeted profiling towards quanti-
 1567 tative metabolomics. *Curr Drug Metab* 13:
 1568 1226–1243
- 1569 183. Chen J, Zhou L, Zhang X et al (2012)
 1570 Urinary hydrophilic and hydrophobic met-
 1571 abolic profiling based on liquid
 1572 chromatography-mass spectrometry meth-
 1573 ods: differential metabolite discovery spe-
 1574 cific to ovarian cancer. *Electrophoresis* 33:
 1575 3361–3369
- 1576 184. Yuan W, Zhang J, Li S et al (2011) Amine
 1577 metabolomics of hyperglycemic endothelial
 1578 cells using capillary LC-MS with isobaric tag-
 1579 ging. *J Proteome Res* 10:5242–5250
- 1580 185. Wei R, Li G, Seymour AB (2010) High-
 1581 throughput and multiplexed LC/MS/MRM
 1582 method for targeted metabolomics. *Anal*
 1583 *Chem* 82:5527–5533
- 1584 186. Grison S, Martin JC, Dublineau I et al (2010)
 1585 Metabolomics, a new approach to identify
 1586 biomarkers of ¹³⁷Cs health effects. *Toxicol*
 1587 *Lett* 196:S54
187. Ciborowski M, Javier Ruperez F, Paz 1588
 Martinez-Alcazar M et al (2010) Metabolomic 1589
 approach with LC-MS reveals significant effect 1590
 of pressure on diver's plasma. *J Proteome Res* 1591
 9:4131–4137 1592
188. An Z, Chen Y, Zhang R et al (2010) 1593
 Integrated ionization approach for 1594
 RR/LC-MS/MS-based metabolomics: find- 1595
 ing potential biomarkers for lung cancer. 1596
J Proteome Res 9:4071–4081 1597
189. Brown SD, Rhodes DJ, Pritchard BJ (2007) 1598
 A validated SPME-GC-MS method for simul- 1599
 taneous quantification of club drugs in human 1600
 urine. *Forensic Sci Int* 171:142–150 1601
190. Hori D, Hasegawa Y, Kimura M et al (2005) 1602
 Clinical onset and prognosis of Asian children 1603
 with organic acidemias, as detected by analysis 1604
 of urinary organic acids using GC/MS, instead 1605
 of mass screening. *Brain Dev* 27:39–45 1606
191. Meyer MR, Peters FT, Maurer HH (2010) 1607
 Automated mass spectral deconvolution and 1608
 identification system for GC-MS screening for 1609
 drugs, poisons, and metabolites in urine. *Clin* 1610
Chem 56:575–584 1611
192. Yoon H-R (2007) Two step derivatization for 1612
 the analyses of organic, amino acids and gly- 1613
 cines on filter paper plasma by GC-MS/ 1614
 SIM. *Arch Pharmacol Res* 30:387–395 1615
193. Kanani H, Chrysanthopoulos PK, Klapa MI 1616
 (2008) Standardizing GC-MS metabolomics. 1617
J Chromatogr B Analyt Technol Biomed Life 1618
Sci 871:191–201 1619
194. Babushok VI, Linstrom PJ, Reed JJ et al 1620
 (2007) Development of a database of gas 1621
 chromatographic retention properties of 1622
 organic compounds. *J Chromatogr A* 1157:
 414–421 1624
195. Kind T, Wohlgemuth G, Lee DY et al (2009) 1625
 FiehnLib: mass spectral and retention index 1626
 libraries for metabolomics based on quadrupole 1627
 and time-of-flight gas chromatography/mass 1628
 spectrometry. *Anal Chem* 81:10038–10048 1629

Author Queries

Chapter No.: 13 0002252423

Queries	Details Required	Author's Response
AU1	Please check whether the affiliations are appropriate as typeset.	OK
AU2	Please check whether edit made to hierarchy of heading levels is appropriate.	OK
AU3	Please check whether the edits made to Tables 1 and 2 are appropriate.	OK
AU4	Please check whether the presentation of list numbers are appropriate.	OK
AU5	Please check if "turrine" should be changed to "taurine".	taurine
AU6	Please note that Refs. [96, 142] have been deleted in original reference list as they are duplicates of Refs. [18, 134], respectively. Therefore the subsequent references and the corresponding citations have been renumbered. Please check.	OK
AU7	Please provide volume number for Ref. [32].	Volume 8
AU8	Please provide page ranges for Ref. [65].	conference poster

Uncorrected Proof